

Boundary Layer Flow with Radiation Heat Transfer and a Hydrolysis Reaction
during the Cu-Cl Cycle of Hydrogen Production

by

Samita Rimal

A Thesis Submitted to the School of Graduate Studies in Partial Fulfillment of the Requirements

for the Degree of

Master of Engineering

in

The Faculty of Engineering and Applied Science

Mechanical Engineering

Memorial University of Newfoundland

February 2024

©Samita Rimal, 2024

Abstract

With the realization of Earth's depleting fossil fuel reserves, the environment-friendly technologies and renewable energy sources has been witnessing a growing demand for. As an energy carrier, hydrogen has emerged as a promising solution aimed at addressing clean energy demands while limiting carbon emissions. Current usage of hydrogen as the carrier of energy is primarily obtained from fossil fuel reformation while releasing CO₂ into the atmosphere. Replacement of hydrocarbon fuels by hydrogen produced from sustainable and cost-effective thermochemical water splitting is a promising technology. The Copper-Chlorine (Cu-Cl) cycle offers a proven and environmentally advantageous method for hydrogen production. This process distinguishes itself through its relatively low heat requirement in comparison to other hydrogen production methods. However, complex solid-gas reactions and heat transfer present challenges that need to be addressed for industrial-scale implementation.

The conversion from cupric chloride (CuCl₂) to copper oxychloride (Cu₂OCl₂) in the hydrolysis stage of the Cu-Cl cycle determines the reaction extent, chemical kinetics of each process and hence the hydrolysis reactor efficiency for industrial scale-up. Numerous investigations have focused on the heat and mass transfer of hydrolysis reactions, aiming to understand their respective roles and enhance the overall cycle efficiency. However, few or no prior research has explored the impact of radiation on the process. This thesis focuses on radiation heat transfer incorporating thermophysical property variation in the hydrolysis step of the cycle to better understand the heat transfer processes inside the reactor.

The primary contribution of this thesis lies in the development of a semi-analytical model that integrates radiative heat transfer and chemical reactions in a gas-solid system, employing a

similarity solution and numerical methods. A similarity transformation is used to solve the governing equations utilizing a fourth-order Runge-Kutta method and a Rosseland approximation is employed to study the impact of thermal radiation.

It is recognized that thermal radiation has a significant role in the boundary layer flow problem in a hydrolysis reaction. The thickness of the thermal boundary layer was observed to increase with the change of radiation parameters. The presence of the chemical reaction thickens the thermal boundary layer and the effect of the endothermic chemical reaction on the thermal boundary layer thickness is found to be decreasing with an increase in the radiation parameter. The solid particle presence enhances the heat and mass transfer and affects the concentration profile. It is also known that the combined influence of thermal radiation and varying thermophysical properties is crucial and reveals a decrease in the concentration of chemical species near the wall surface. This could be due to enhanced mass transfer, an increase in the reaction rate, or changes in fluid properties with temperature in promoting faster diffusion of species away from the boundary.

The result of this study provides valuable insight into the effects of radiation and chemical reactions on the boundary layer behaviour. A better comprehension of the thermal radiation effects in the flow in the hydrolysis reaction will be beneficial to improve the reactor design in the thermochemical cycle of hydrogen production while improving the overall Cu-Cl cycle efficiency. Overall, this research presented a detailed boundary layer study with hydrolysis along a flat surface and highlighted the effects of thermal radiation and thermophysical property variations.

Author's Declaration

I hereby declare that this thesis consists of the original work that I have authored. I grant Memorial University of Newfoundland permission to reproduce, whether through photocopying or other means, the entirety or partial content of this work upon request from other institutions or individuals for research purposes. I also acknowledge that this study will be made electronically accessible to the public.

Samita Rimal

Samita Rimal

Acknowledgement

I would like to express my gratitude to my supervisors Dr. K. Pope, Dr. G. F. Naterer, and Dr. K. A. Hawboldt for their continued support and guidance during this research. Their expert advice and excellent leadership have been invaluable throughout all stages of work.

I would like to thank Memorial University of Newfoundland for providing excellent working conditions. Acknowledgments are extended to the Canadian Nuclear Laboratories (CNL) and Natural Sciences and Engineering Research Council of Canada (NSERC) for their financial support.

Table of Contents

Abstract.....	ii
Author’s Declaration.....	iv
Acknowledgement	v
Table of Contents.....	vi
Nomenclature.....	ix
Greek Symbols.....	x
Acronyms.....	x
Subscripts.....	xi
List of Figures.....	xii
List of Tables	xiii
Co-Authorship Statement.....	xiv
Chapter 1 – Introduction.....	1
1.1 Global Challenge	1
1.2 Boundary Layer Flow	5
1.3 Scope and Objectives of Thesis	6
1.4 Thesis Structure	7
References.....	8
Chapter 2 – Literature Survey	11

2.1 Cu-Cl Cycle Overview.....	11
2.2 Hydrolysis Reaction.....	14
2.3 Boundary Layer Flow and Heat Transfer	16
2.4 Conclusions.....	17
References.....	18
Chapter 3 – Radiation Effects on a Chemically Reacting Flow with Hydrolysis	25
Abstract.....	25
3.1 Introduction.....	26
3.2 Mathematical Problem Formulation	28
3.3 Modeling.....	32
3.3.1 Similarity Transformation.....	32
3.3.2 Governing ODEs.....	33
3.4 Results and Discussion	34
3.4.1 Results.....	34
3.4.2 Validation.....	38
3.5 Conclusions.....	40
References.....	41
Chapter 4 – Solid-Gas Flow with Variable Thermophysical Properties	43
Abstract.....	43
4.1 Introduction.....	44

4.2 Governing Equations	47
4.3 Case Studies	53
4.3.1 Case I	53
4.3.2 Case II	54
4.3.3 Case III.....	56
4.4 Results and Discussion	57
4.5 Conclusions.....	69
References.....	70
Chapter 5 – Conclusions and Recommendations	77
5.1 Future Recommendations	78
Appendix A: MATLAB Codes.....	81
Maximum Radiation Model ($NR = 0.3$) – Function and Script.....	81
Plots.....	83

Nomenclature

b	=	Stoichiometric reaction coefficient
C	=	Solid particle concentration (mol/m ³)
C_p	=	Specific capacity (J/kg·K)
C_∞	=	Ambient steam concentration (mol/m ³)
D	=	Effective diffusion coefficient (m ² /s)
f	=	Dimensionless stream function
ΔH	=	Heat of reaction of endothermic reaction (kJ/mol)
k_1	=	Chemical reaction constant (mol/m ³ ·s)
N_R	=	Radiation Parameter
Nu	=	Nusselt number
Pr	=	Prandtl number
q_r	=	Radiative heat flux (W/m ²)
Re	=	Reynolds number
R_H^*	=	Reaction heat parameter (mol·s ² /m ³)
Sc	=	Schmidt number
T	=	Temperature (K)
u	=	Velocity components in the x direction (m/s ²)

U_{∞} = Constant free stream velocity away from the surface (m/s²)

v = Velocity component in the y direction (m/s²)

Greek Symbols

α = Thermal diffusivity (m²/s)

γ = Relative temperature difference parameter

η = Similarity variable

θ = Dimensionless temperature

k = Thermal conductivity (W/m·K)

k^* = Mean absorption coefficient (m²/mol)

μ = Dynamic viscosity (N·s/m²)

ν = Kinematic viscosity (m²/s)

ρ = Total density of the participating gas-solid mixture (kg/m³)

σ = Stefan-Boltzmann constant (W/m²·K⁴)

ϕ = Dimensionless concentration

ψ = Stream function

ω = Solid particle mass fraction

Acronyms

CCUS = Carbon Capture, Usage and Storage

Cu-Cl = Copper Chlorine
GHG = Green House Gases
MF = Mass fraction
ODE = Ordinary Differential Equation
PDE = Partial Differential Equation
SMR = Steam Methane Reforming
TPV = Variable thermophysical property
TWSC = Thermochemical Water Splitting Cycles

Subscripts

f = Fluid
 g = Gas
 l = Liquid
 s = Solid
 w = Wall
 ∞ = Free stream

List of Figures

Figure 1.1 Schematic diagram of the four-step copper-chlorine cycle 4

Figure 2.1 Schematic of the 4-step Cu-Cl Hydrogen Production Cycle 13

Figure 3.1 Geometry of the problem..... 29

Figure 3.2 Comparison of numerical method with Bataller [6] 39

Figure 3.3 Temperature distribution across boundary layer as a function of η for cases with radiation ($N_R = 0.3, 0.7$ and 1) and without radiation ($k_0 = 1$) 35

Figure 3.4 Temperature gradient across boundary layer as a function of η for cases with radiation ($N_R = 0.3, 0.7$ and 1) and without radiation ($k_0 = 1$) 36

Figure 3.5 Concentration profile as a function of η for radiation case, $N_R = 0.7$ 37

Figure 4.1 Velocity profile including thermophysical property variations and mass fraction of the mixture as a function of η in the presence of radiation ($N_R = 0.3$ and 1) and absence of radiation ($k_0 = 1$) 58

Figure 4.2 Temperature profile as a function of η including thermophysical property variations and mass fraction of the mixture in the presence of radiation ($N_R = 0.3$ and 1) and absence of radiation $k_0 = 1$ 60

Figure 4.3 Temperature gradient across a boundary layer including thermophysical property variations and mass fraction of the mixture in the presence of radiation ($N_R = 0.3$ and 1) and absence of radiation $k_0 = 1$ 61

Figure 4.4 Concentration profile trends with respect to η including thermophysical property variations and mass fraction of the mixture in the presence of radiation ($N_R = 0.3$ and 1) and absence of radiation $k_0 = 1$ 63

Figure 4.5 Velocity profile with varying solid particle mass fraction for a maximum radiation case..... 64

Figure 4.6 Concentration profile in the boundary layer with varying solid particle mass fraction for a maximum radiation case 65

Figure 4.7 Temperature gradient across a boundary layer with varying solid particle mass fraction for a maximum radiation case 66

Figure 4.8 Velocity profile across a boundary layer with varying Prandtl number at $k_0 = 1$ and $N_R = 0.3$	67
Figure 4.9 Concentration profile across a boundary layer with varying Prandtl number at $k_0 = 1$ and $N_R = 0.3$	68
Figure 4.10 Temperature profile across a boundary layer with varying Prandtl number at $k_0 = 1$ and $N_R = 0.3$	69

List of Tables

Table 1.1 Hydrogen Production techniques worldwide as of 2022 [8].....	3
Table 2.1 Thermochemical Cycles for Hydrogen Production	12
Table 3.1 Validation of numerical model	40
Table 3.2 Values of the rate of heat transfer $\theta'(0)$ and the rate of mass transfer $\phi'(0)$	38
Table 4.1 Heat transfer in flow along a plate represented as the local heat transfer parameter ($NuxRex - 1/2$)	62

Co-Authorship Statement

The author of this thesis, Samita Rimal, was primary author for all corresponding published papers, and conducted the numerical modeling and analysis. Dr. Kevin Pope and Dr. Greg F. Naterer served as the principal supervisors, offering technical guidance, analytical support, supervision and editing. They are co-authors for published papers related to Chapters 3 and 4. Furthermore, Dr. Kelly A. Hawboldt provided technical guidance, analytical support, and editing of papers related to Chapters 3 and 4 and is a co-author of the corresponding papers.

The chapters that are based on these publications are listed here and their findings are highlighted in some chapters here.

- The understanding of boundary layer heat and mass transfer incorporating thermal radiation effects and chemical reactions is introduced in Chapter 3. The existing model is validated with a previous study.
- A major part of Chapter 4 was submitted to a journal. This chapter presents the analysis of the hydrolysis reaction and radiation in a solid-gas flow with variable thermophysical properties.

Chapter 1 – Introduction

1.1 Global Challenge

The Earth naturally imposes limits on the resources available to us, with the exception of the continuous supply of energy from the sun. Historically, human resource consumption remained within the planet's regenerative capacity until the 20th century. However, significant technological advancements, resulting in improved living standards and a rapid global population increase, have led to a sharp increase in annual resource consumption. This surge has surpassed the Earth's ability to renew these resources [1]. One illustrative example of this disparity is the concept of Earth Overshoot Day, which signifies the point where our consumption exceeds the planet's ability to replenish. In the 1970s, this day fell at the end of December, but it now occurs in mid-July, indicating that humanity's consumption is equivalent to 1.7 Earths instead of just one [1].

The escalating global resource consumption and the associated rise in fossil fuel usage have long been areas of concern. Fossil fuel consumption is a primary driver of climate change, responsible for roughly 70% of greenhouse gas emissions like CO₂, CH₄, and NO_x [2]. As we currently consume resources, global fossil fuel reserves are depleting rapidly, with projections suggesting significant reductions in oil and gas reserves within the next 35 to 50 years [3, 4]. This situation underscores the urgent need for cleaner and more efficient production methods that integrate sustainable energy sources, with the aim of eventually replacing or complementing existing processes [5].

Hydrogen energy possesses several key attributes that make it a favorable clean energy carrier. Being light, energy-dense, storable and producing no direct emissions, hydrogen can be produced from low or zero carbon sources such as nuclear, solar, water, and biomass [5]. It has an advantage

of existing as an energy carrier as well as energy storage medium. It can be used in a wide range of applications as a significant alternative to current fuels, or to complement the greater use of electricity, for transport, steel production, heating, or for hydrogen-based fuels [5, 6]. It is acknowledged as an environmentally friendly option when employed as an energy source, offering the potential to address a range of pressing energy challenges, including transportation and air quality, while bolstering energy security on a broader scale [6, 7]. Additionally, hydrogen plays a pivotal role in an array of products that contribute to various industries and societal needs, including fertilizers, pharmaceuticals, metallic materials, and construction supplies.

A recent report has shown that the demand for hydrogen has grown more than threefold in the past 50 years [6]. In 2022, worldwide hydrogen production nearly reached 95 million metric tons, showing a 3% growth compared to the previous year, 2021 [8]. Hydrogen ranks as the third most abundant element on Earth, predominantly occurring in water (H_2O) and within organic compounds, fossil fuels, and biomass. Consequently, when harnessing hydrogen for various applications, it needs to be generated from these larger molecules. At present, the leading method for hydrogen production is steam methane reforming (SMR) of natural gas. This is followed by coal gasification and partial oxidation techniques [6]. In the endothermic SMR process, methane from natural gas is reacted with steam to produce hydrogen in the presence of a catalyst. However, it's worth noting that this method results in the release of 10 - 13 kg of CO_2 equivalent emissions for each kilogram of net hydrogen produced [9 - 11]. Utilizing coal gasification for the production of hydrogen involves converting coal into synthetic gas using water vapour but this method produces twice as much carbon emissions compared to SMR [6].

Currently, hydrogen is almost entirely supplied from fossil fuels. Hydrogen production is responsible for around 830 million tonnes of CO_2 production per year [6]. In 2022, there was a 3%

increase in global hydrogen production, reaching 95 million metric tons. However, the production of low-emission hydrogen constituted less than 1% of the total production [8]. Despite the fact that carbon capture methods can be used to reduce emissions from aforementioned hydrogen production methods, it has been deemed important to study the clean methods for producing hydrogen. Table 1.1 showcases the current trend of hydrogen production worldwide with the low emission hydrogen production contributing to only 0.7% of global production in 2022.

Table 1.1 Hydrogen Production techniques worldwide as of 2022 [8]

No.	Production Technology	Percentage (%)
1.	Natural gas w/o CCUS	62
2.	Coal	21
3.	By-product hydrogen	16
4.	Fossil fuels with CCUS	0.6
5.	Oil	0.5
6.	Electricity	0.1

Thus, low emission pathways have been extensively studied to address current greenhouse gas (GHG) emission issues related with hydrogen production. Biomass gasification, thermochemical water splitting, and solar water splitting are some of the methods providing a lower emission pathway to the production of hydrogen. Thermochemical water splitting cycles (TWSC) have been established as a sustainable option for hydrogen production. These cycles are water-splitting cycles that divide the water molecule into streams of hydrogen and oxygen gas through a series of close sequence chemical reactions [5]. Over 200 types of thermochemical cycles have been studied in the past with the Cu-Cl cycle being identified as the most viable one due to its advantages over

other thermochemical processes due to its economic and scientific feasibility including greater simplicity, lower temperature requirements between 500°C and 600 °C, and lower capital costs [5, 7, 12 - 14]. Other advantages of this cycle include the utilisation of waste heat for hydrogen production [13].

Different variations of the Cu-Cl cycle can be found in past literature, namely, two-step, three-step, four-step, and five-step cycles [5, 15]. The four-step process is the most common. Figure 1.3 presents the interactions between the four steps. It offers considerable advantages in chemical kinetics, solid handling and lower process complexity as compared with other cycles [15, 16].

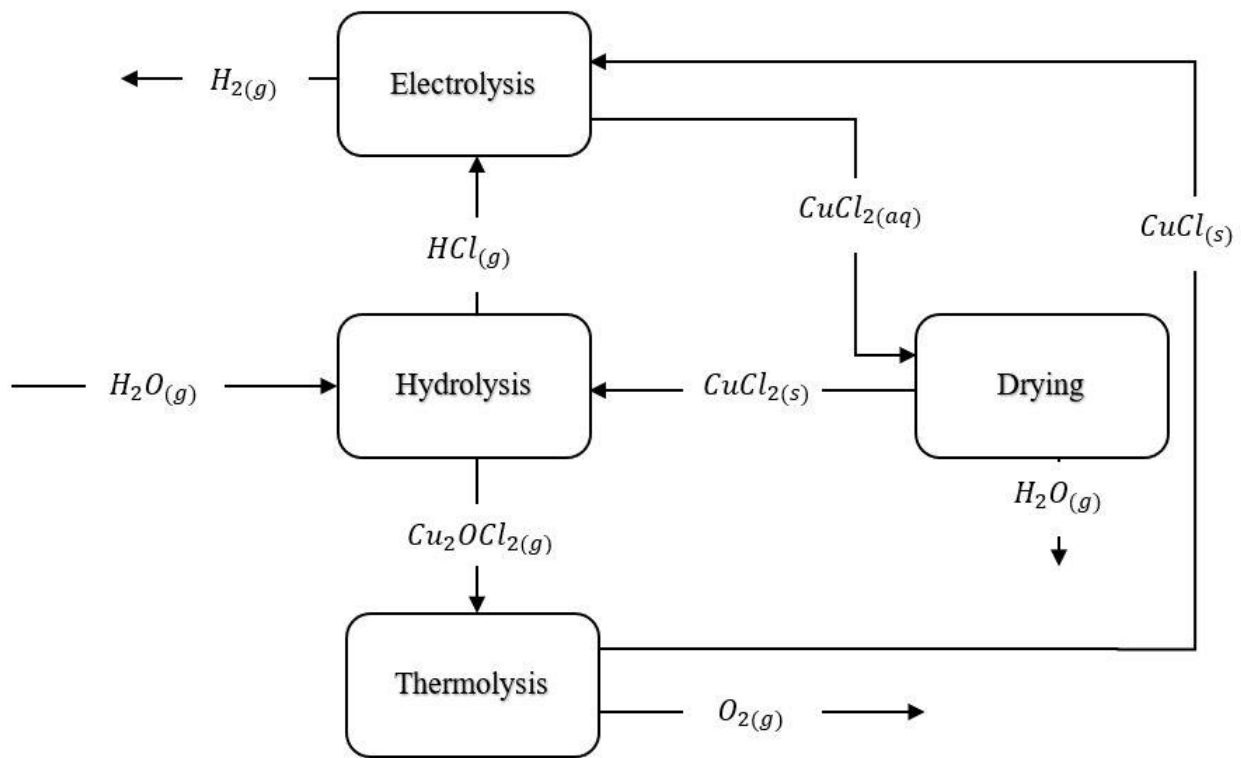


Figure 1.1 Schematic diagram of the four-step copper-chlorine cycle

Hydrolysis step presents a significant challenge for attaining higher efficiency in the system due to side reactions and excess steam requirements [5, 16, 17]. A strict temperature range of 375 - 400 °C is required for the hydrolysis reaction to attain maximum conversion of solid copper chloride particles in the reaction for improved efficiency. A proper understanding of heat transfer inside the reactor is crucial since higher reactant temperature fuels undesired side reactions [16, 18]. This thesis presents examines heat and mass transfer in the hydrolysis step of the Cu-Cl cycle which is a part of the larger global challenge of hydrogen production in a sustainable manner to reduce emissions and environmental impacts.

1.2 Boundary Layer Flow

Boundary layer flow diffusion is a critical phenomenon in fluid dynamics that plays a pivotal role in understanding heat and mass transfer processes [19]. In the context of fluid mechanics, the boundary layer refers to the thin layer of fluid adjacent to a solid surface where the fluid velocity changes from zero at the surface to the free-stream velocity. This layer region is characterized by the development of both momentum and thermal boundary layers, each influencing the heat and mass transport phenomena.

The momentum boundary layer is a region where the velocity of the fluid gradually increases from zero at the solid surface to the free-stream velocity [19]. Understanding the characteristics of the momentum boundary layer is essential for predicting drag forces, shear stresses, and overall fluid behavior near solid surfaces. Thermal boundary layer involves the gradual transition of temperature from the surface to the bulk fluid, influencing heat transfer mechanisms [20]. Studying both the momentum and thermal boundary layers are crucial in comprehending the complexities have significance in heat and mass transfer phenomena in chemical processes like hydrolysis.

Understanding the thermal boundary layer is crucial for gaining insight into heat and mass transfer dynamics in temperature-sensitive reactions, such as hydrolysis. In this thesis, the study of boundary layer flow with an emphasis on radiation heat transfer and in a hydrolysis reaction of relevance to the Cu-Cl thermochemical cycle during the cu-cl hydrogen production cycle is presented. Further details on boundary layer fluid flow and heat transfer are presented in Section 2.3.

1.3 Scope and Objectives of Thesis

Embedded in this global context, it is the objective of this thesis to study heat and mass transfer during the hydrolysis step in the copper-chlorine cycle. A comprehensive investigation into heat transfer, particularly regarding thermal radiation, is a useful contribution to the study of hydrolysis reactions. This is noteworthy because while radiation effects in flows with chemical reactions and solid particles have been extensively explored [21 - 24], a comprehensive examination of such effects in the context of hydrolysis reactions is absent.

To enhance the overall system efficiency, it is crucial to effectively design and control the chemical reactors within the Cu-Cl cycle. The outcome of this research brings forth new insights, including the development of a radiation heat transfer model for the hydrolysis step which is a novel contribution to the field. This can be utilized in the development of labs and industrial-scale hydrolysis reactors. Results for the boundary layer heat transfer effects in the reactor are presented which offer useful insight into the reactor operation and design. The cumulative impact of this work aims to advance hydrolysis reactor optimization in the thermochemical Cu-Cl cycle, given the high temperature sensitivity of the hydrolysis process. Understanding radiation heat transfer effects in the boundary layer helps analyze the ways to improve the reactor design incorporating real-world conditions.

The primary objectives of this thesis are outlined as follows:

- Identify the impact of radiation heat transfer in the thermal boundary layer and fluid flow.
- Study the influence of the hydrolysis reaction in the thermal boundary layer via numerical modelling.
- Determine the effects in the boundary layer caused by temperature dependent thermophysical properties.

1.4 Thesis Structure

Chapter 2 provides the theoretical foundation of this thesis with a review of relevant literature surrounding the thermochemical Cu-Cl water splitting cycle and transport phenomena during the step. In this chapter, a review begins with different variations in the Cu-Cl cycle and hydrolysis reaction. Additional elaboration on the heat transfer and fluid flow with gas-solid reactions is presented based on previous studies and research. This review leads to an investigation of the use of numerical modeling for studying thermal radiation effects in the thermal boundary layer of the hydrolysis step. Chapter 3 discusses mathematical problem formulation. The nature of the problem is explained with the results and model validated with a past study. A major section in this chapter has been presented in conference proceedings and was accepted for publication.

Chapter 4 builds on the previously established results from Chapter 3. The validated model is used for further study of an endothermic hydrolysis reaction including solid particles and temperature dependent properties. Under a maximum radiation condition, further sensitivity analysis is carried out to identify optimal parameters to achieve maximum heat and mass transfer and overall efficiency. This chapter has also been submitted for publication. Chapter 5 summarizes the major

findings and interprets the results. Concluding remarks and recommendations for future studies are provided to conclude the thesis.

References

- [1] M. Wackernagel, and S. Browne, "Earth overshoot day," Accessed: Aug. 17, 2023. [Online]. Available: overshootday.org.
- [2] J. Lelieveld, K. Klingmüller, A. Pozzer, R. T. Burnett, A. Haines, and V. Ramanathan, "Effects of fossil fuel and total anthropogenic emission removal on public health and climate," *Proceedings of the national academy of sciences U. S. A.*, vol. 116, no. 15, pp. 7192 - 7197, 2019.
- [3] S. Shafiee, and E. Topal, "When will fossil fuel reserves be diminished?," *Energy policy*, vol. 37, no. 1, pp. 181 - 189, 2009.
- [4] G. Boyle, B. Everett, S. Peake, and J. Ramage, "Energy systems and sustainability: Power for a sustainable future," *Second Oxford: Oxford University Press*, 2012.
- [5] G. F. Naterer, I. Dincer, and C. Zamfirescu, "Hydrogen production from nuclear energy," 2013.
- [6] International Energy Agency, "The future of hydrogen," 2019.
- [7] G. Naterer *et al.*, "Recent Canadian advances in nuclear-based hydrogen production and the thermochemical Cu-Cl cycle," *International journal of hydrogen energy*, vol. 34, no. 7, 2009.
- [8] International Energy Agency, "*Global hydrogen review*," 2023.
- [9] B. Chen, Z. Liao, J. Wang, H. Yu, and Y. Yang, "Exergy analysis and CO₂ emission evaluation for steam methane reforming," *International journal of hydrogen energy*, vol. 37, no. 4, pp. 3191 - 3200, 2012.

- [10] F. Suleman, I. Dincer, and M. Agelin-Chaab, "Environmental impact assessment and comparison of some hydrogen production options," *International journal of hydrogen energy*, vol. 40, no. 21, pp. 6976 - 6987, 2015.
- [11] P. Spath, and M. Mann, "Life cycle assessment of hydrogen production via natural gas steam reforming," 2003.
- [12] B. W. Mcquillan *et al.*, "High efficiency generation of hydrogen fuels using solar thermal-chemical splitting of water (Solar thermo-chemical splitting for H₂)," 2010.
- [13] K. Pope, "*Multiphase flow and chemical reactor thermodynamics for hydrolysis and thermochemical hydrogen production*," 2012.
- [14] C. Zamfirescu, I. Dincer, and G. F. Naterer, "Thermophysical properties of copper compounds in copper-chlorine thermochemical water splitting cycles," *International journal of hydrogen energy*, vol. 35, no. 10, pp. 4839 - 4852, 2010.
- [15] M. F. Orhan, I. Dinçer, and M. A. Rosen, "Efficiency comparison of various design schemes for copper-chlorine (Cu-Cl) hydrogen production processes using Aspen Plus software," *Energy conversion and management*, vol. 63, pp. 70 - 86, 2012.
- [16] A. Farsi, I. Dincer, and G. F. Naterer, "Review and evaluation of clean hydrogen production by the copper-chlorine thermochemical cycle," *Journal of cleaner production*, vol. 276, p. 123833, 2020.
- [17] V. N. Daggupati, G. F. Naterer, K. S. Gabriel, R. J. Gravelins, and Z. L. Wang, "Equilibrium conversion in Cu-Cl cycle multiphase processes of hydrogen production," *Thermochemical Acta*, vol. 496, no. 1 - 2, pp. 117 - 123, 2009.

- [18] V. N. Daggupati, G. F. Naterer, and K. S. Gabriel, "Diffusion of gaseous products through a particle surface layer in a fluidized bed reactor," *International journal of heat mass transfer*, vol. 53, no. 11 - 12, pp. 2449 - 2458, 2010.
- [19] H. Schlichting and K. Gersten, "Boundary-Layer Theory", *9th ed. Springer*, 2016.
- [20] F. P. Incropera and D. P. DeWitt, "Fundamentals of Heat and Mass Transfer", *6th ed. John Wiley & Sons*, 2006.
- [21] P. K. Tripathy, T. Samantara, J. Mishra, and S. Panda, "Mixed convective radiative heat transfer in a particle-laden boundary layer fluid over an exponentially stretching permeable surface," *AIP conference proceedings*, vol. 2435, 2022.
- [22] W.J. Smith, "Effect of gas radiation in the boundary layer on aerodynamic heat transfer," *Journal of the aeronautical sciences*, vol. 20, pp. 579 - 580, 1952.
- [23] R. Viskanta, and R. J. Grosh, "Boundary layer in thermal radiation absorbing and emitting media," *International journal of heat and mass transfer*, vol. 5, no. 9, pp. 795 - 806, 1962.
- [24] A. J. Chamkha, and J. Peddieson Jr, "Boundary layer flow of a particulate suspension past a flat plate," *International journal of multiphase flow*, vol. 17, pp. 805 - 808, 1991.

Chapter 2 – Literature Survey

The objective of this literature review is to present a comprehensive understanding of existing scholarly works and achievements in the development of the thermochemical Cu-Cl cycle, hydrolysis reactor kinetics, heat and mass transfer analysis, and fluid flow with chemical reaction. Past understanding of the hydrolysis reactor and boundary layer transport phenomena are discussed in this chapter. Previous scientific research along with existing achievements and the critical requirements associated with improving cycle efficiency are discussed.

2.1 Cu-Cl Cycle Overview

In thermochemical water splitting cycles, water is decomposed into hydrogen and oxygen in a sequence of chemical reactions in a closed system [1 - 3]. Brown et al. [4] and McQuillan et al. [5] have documented the high-efficiency generation of hydrogen through thermochemical methods, where nuclear power or solar energy serves as the heat source in their respective studies. Among the 200 variations of the feasible cycles, only a few of them have the potential of being economically and technically viable [6]. Table 2.1 outlines several feasible thermochemical cycles that have been examined in previous literature, along with the typical operating temperature ranges [7 - 12].

The copper-chlorine cycle stands out among the various thermochemical cycles for large-scale hydrogen production, primarily due to its relatively lower temperature requirements, a significant advantage in comparison to other high-temperature-dependent processes [3, 6, 13, 14]. This lower temperature demand presents an opportunity for more efficient integration with nuclear power stations, allowing the utilization of waste heat generated by next-generation Supercritical Water-Cooled Reactors (SWCR) or other renewable energy sources [3, 15].

Table 2.1 Thermochemical Cycles for Hydrogen Production

No.	Type	Max. Temperature	Source
1	Sulfur Iodine	>800 °C	Kubo <i>et al.</i> [7]
2	Hybrid Sulfur	900 °C	Sattler <i>et al.</i> [8]
3	Magnesium Iodine Cycle	600 °C	Shindo <i>et al.</i> [9]
4	Cerium Chlorine Cycle	730 °C	Lemont <i>et al.</i> [10]
5	Iron Chlorine	925 °C	Safari <i>et al.</i> [11]
6	Copper Chlorine Cycle	<550 °C	Naterer <i>et al.</i> [12]

Other advantages of the Cu-Cl cycle include more simplicity, higher overall conversion efficiency, and lower maintenance due to low temperature requirement, no catalyst requirement and readily available chemical species. Various research initiatives conducted by institutions like the Argonne National Laboratory (ANL), Pennsylvania State University (PSU), Canadian Nuclear Laboratories (CNL), and UOIT have made substantial contributions to the scaling up of the Cu-Cl cycle for industrial applications [14].

Ferrandon *et al.* [16] outlined the Cu-Cl cycle, highlighting its three primary stages: electrolysis, hydrolysis, and decomposition (thermolysis). Farsi *et al.* [17] identified four reaction steps during their study of the hydrolysis stage while Daggupati *et al.* [18] presented a five-step cycle based on thermodynamic equilibrium analysis. Two independent studies by Orhan *et al.* [19] and Ozbilen *et al.* [20] evaluated the exergy, energy, yield effectiveness, and the overall Life Cycle Assessment (LCA) and established the 4-step cycle as the most efficient technique with a maximum system efficiency of 36% amongst the 2-step, 3-step, and 5-step Cu-Cl cycle [6, 13]. Figure 2.1 presents a schematic of the Cu-Cl thermochemical cycle.

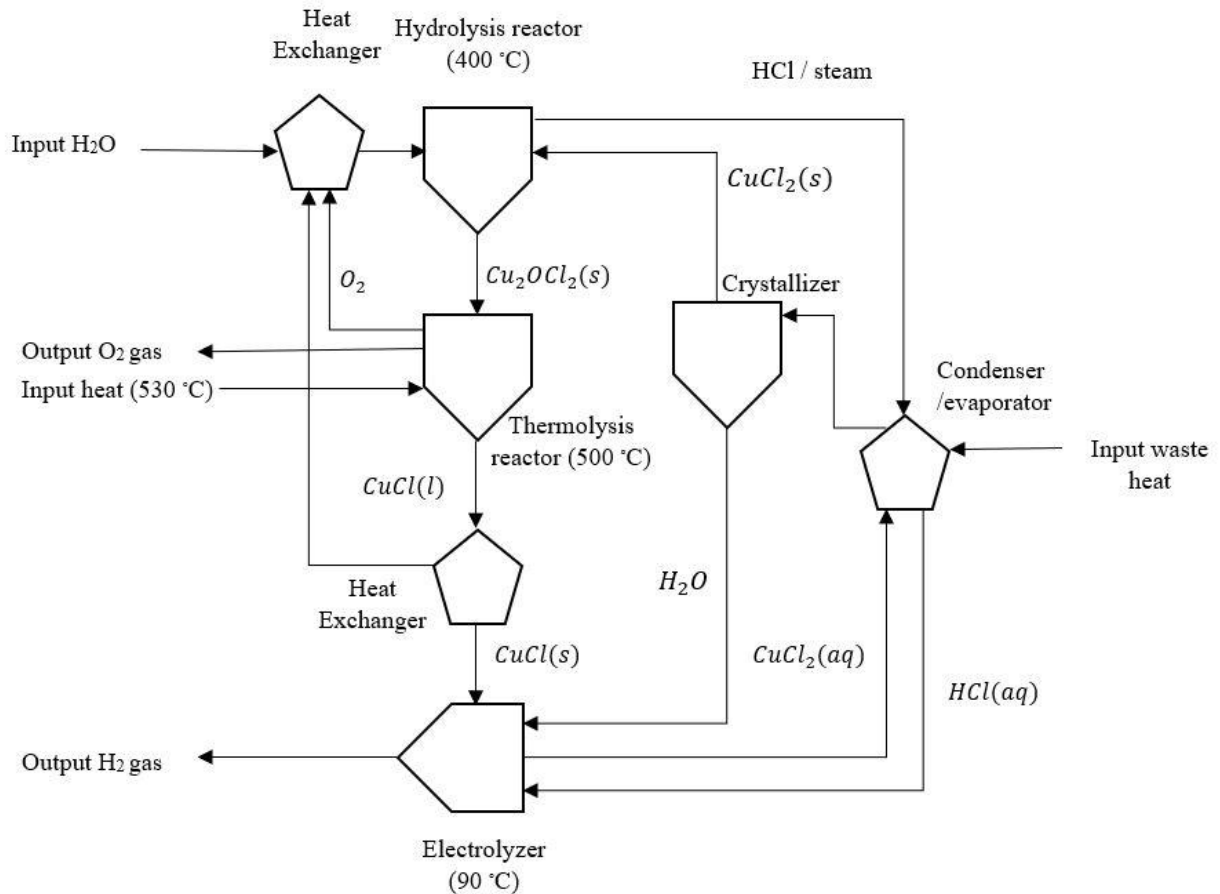
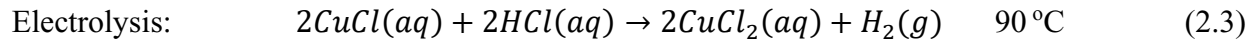
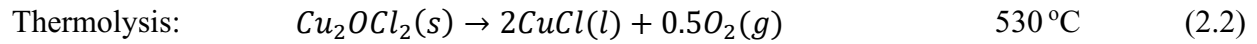
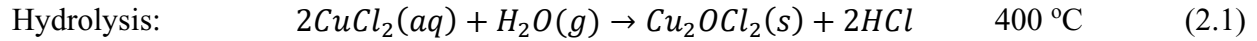


Figure 2.1 Schematic of the 4-step Cu-Cl Hydrogen Production Cycle

In the four-step cycle, the integration of three reaction systems - namely, hydrolysis, thermolysis, and electrolysis - with a drying process enables the separation of water into hydrogen and oxygen. The process works in a loop by continually utilizing the internal chemicals as illustrated in Fig. 2.1, which makes the thermochemical cycles more promising and efficient. The chemical reactions occurring in the four-step Cu-Cl cycle along with their temperature requirements are presented represented in equations (2.1) to (2.4).



Improvement of each step will lead to substantial progress towards an efficiently integrated cycle [13, 23]. Notably, the hydrolysis reaction presents a considerable challenge in achieving higher system efficiency, primarily due to its exacting temperature requirements [1, 16, 17, 24]. The focus of this research to contribute to the step will be discussed in the upcoming sections.

2.2 Hydrolysis Reaction

In the hydrolysis reaction, solid $CuCl_2$ and steam mixture react to form copper oxychloride (Cu_2OCl_2) and hydrogen chloride (HCl). It is an endothermic, non-catalytic gas-solid reaction occurring at a temperature of approximately 400 °C. The non-catalytic gas-solid hydrolysis reaction is represented by Equation (2.1). Increased efficiency of the hydrolysis step is crucial for attaining higher overall Cu-Cl cycle efficiency. Three levels for the efficiency calculation are defined by Lewis et al. [25]. Level 1 considers the energy required for the proposed cycle, the factors related to equilibrium phases and side reactions are incorporated in Level 2, and Level 3 introduces actual product distribution based on experimental data. The endothermic hydrolysis reaction is a highly temperature sensitive reaction. Despite the desired product being copper oxychloride, Cu_2OCl_2 , and hydrogen chloride, HCl, at a higher reactant temperature, undesired side reactions occur. Maximizing solid conversion is critical for addressing integration complexities with the cycle. However, the same conditions that promote high conversion rates also

facilitate undesired side reactions, leading to the production of potentially hazardous secondary products. Table 2.2 provides a compilation of desired and potential side reactions in a CuCl_2 hydrolysis reactor.

Table 2.2 List of desired and possible side reactions in a CuCl_2 hydrolysis process

No.	Reaction	Remarks
1	$2\text{CuCl}_2(s) + \text{H}_2\text{O}(g) \rightarrow \text{Cu}_2\text{OCl}_2(s) + 2\text{HCl}(g)$	Desired hydrolysis reaction
2	$\text{Cu}_2\text{OCl}_2(s) \rightarrow 2\text{CuCl}(s, l, g) + 0.5\text{O}_2(g)$	Thermolysis of copper oxychloride
3	$\text{Cu}_2\text{OCl}_2(s) \rightarrow \text{CuO} + \text{CuCl}_2(g)$	Copper oxychloride decomposition
4	$\text{CuO} + \text{Cl}_2 \rightarrow \text{CuCl}_2 + 0.5\text{O}_2$	Copper chloride generation
5	$\text{CuCl}_2(s) \rightarrow \text{CuCl}(s, l, g) + 0.5\text{Cl}_2(g)$	Thermolysis of CuCl_2 with CuCl formation
6	$\text{CuCl}_2(s) + \text{CuCl}(s) \rightarrow \text{CuCl}_2/\text{CuCl}(l)$	CuCl_2 / CuCl reaction
7	$3\text{CuCl}(g) \rightarrow \text{Cu}_3\text{Cl}_3(g)$	Formation of tri-copper tri-chloride
8	$\text{CuCl}(s) \rightarrow \text{CuCl}(l)$	Melting of CuCl
9	$\text{Cl}_2(g) + \text{H}_2\text{O}(g) \rightleftharpoons 0.5\text{O}_2(g) + \text{HCl}(g)$	Reverse Deacon and Deacon reactions

All the reactions take place in a hydrolysis reactor. The decomposition of CuCl_2 which generates chlorine and cuprous chloride is the most common and important undesirable reaction inside the hydrolysis reactor. Various hydrolysis reactor types, including a packed bed, fluidized bed, moving bed, and spray reactor, have been developed and examined to mitigate undesired side reactions [3, 16, 26, 27]. In any reactor design, a comprehensive review of the temperature sensitivities within the reactor is crucial for enhancing its efficiency. This is particularly significant in a reactor where multiple reaction pathways are feasible, and their outcomes are highly dependent on temperature variations.

To better set the operating parameters during experimental operation, and to design a more efficient hydrolysis reactor, modelling and simulation play a vital role [3]. Lewis et al. [25] discussed that suitable engineering design should ensure that the temperature in the hydrolysis reactor is maintained within the range of approximately 600 to 700 K. This research presents a detailed understanding of heat transfer modeling in the boundary layer of the reactor whose results can be utilized when designing the highly temperature sensitive hydrolysis reactor in a real-world scenario.

2.3 Boundary Layer Flow and Heat Transfer

Heat transfer and fluid flow processes need to be well understood in the hydrolysis step to accurately predict the reaction extent in the process. Heat and fluid flow with chemical reactions play a critical role for future reactor scale up and development of different variations of experimental reactors [13]. There are several factors which influence the heat transfer in a participating solid-gas flow. In earlier studies concerning heat and fluid flow in hydrolysis, radiation was usually overlooked but there are past studies reporting significant thermal radiation effects in a medium.

Past studies of thermal radiation in a boundary layer flow were discussed by Smith [2]. The effects of thermal radiation on heat transfer in a medium that both absorbs and emits energy were reported by Viskanta and Grosh [3]. Howe [30] and Kadanoff [31] showed that thermal radiation has a potential to influence heat transfer through direct and indirect mechanisms. Radiative heat transfer encompasses the direct absorption or emission of radiation by a surface. Within a boundary layer, some of the thermal radiation may be partially absorbed, resulting in variations in temperature distribution and subsequent effects on heat transfer [29, 32]. Two-dimensional thermal boundary layers around different geometries such as wedge, flat surface, or axisymmetric body have been

extensively examined [33 - 37]. The flow characteristics of fluids within a boundary layer over a stretching surface or wall, both in the presence and absence of thermal radiation, were documented in previous studies [36, 38 - 41].

Earlier studies have also examined the heat transfer effects and boundary layer flows in the presence of chemical reactions with, or without, thermal radiation effects [37, 41 - 44]. Previous investigations by Chamkha et al. [34], as well as Mishra and Tripathy [35, 45], presented analytical and numerical solutions for flows involving multiple phases. Similarly, in the presence of chemical reactions in a solid-gas flow, the overall reactant conversion rate in a chemically reacting flow can be substantially affected by the mass and heat transfer rates [46]. Gireesha et al. [47 - 49] and Sohn et al. [50] have demonstrated the significance of a particle cloud to control the radiative heat flow.

2.4 Conclusions

Hydrogen is a promising pathway to meet the increasing energy demand while reducing global emissions. Currently, steam-methane reforming and coal gasification play a significant role in hydrogen generation. But these techniques contribute to global CO₂ emissions, offsetting the advantages of hydrogen as a clean fuel. Researchers have explored alternative and environmentally friendly production methods, and among these, thermochemical water splitting cycles offer a promising avenue for generating clean hydrogen. While there are numerous thermochemical cycles for hydrogen production, only a handful have met the criteria for large-scale implementation as determined by various assessments.

Among these practical approaches, the Cu-Cl thermochemical cycle stands out due to its lower process temperatures, the ready availability of necessary materials, and its potential integration with waste heat sources. A primary challenge in scaling up the Cu-Cl cycle lies in improving the

efficiency of the hydrolysis step as a highly temperature sensitive step. Previous studies have investigated ways to better understand the heat and mass transfer during the hydrolysis reactor with a focus on experimental studies. Through research it was concluded that heat and mass transfer of the hydrolysis step incorporating thermal radiation has been relatively unexplored area. Additionally, there are limited past predictive models that analyze boundary layer heat transfer and fluid flow with radiation, variable thermophysical properties and chemical reactions. Detailed understanding of these topics can aid in the reactor design to have a better control on the operating temperature and mitigate undesired side reactions.

This research identified potential areas of improvement in the heat and mass transfer during the hydrolysis stage. It has presented a new predictive heat and mass transfer model with the copper-chloride decomposition reaction in the hydrolysis reactor during the thermochemical Cu-Cl cycle. A numerical model outlining the boundary layer heat and fluid flow in the hydrolysis step with thermal radiation effects was presented.

References

- [1] G. F. Naterer, I. Dincer, and C. Zamfirescu, "Hydrogen production from nuclear energy," 2013.
- [2] G. F. Naterer *et al.*, "Recent Canadian advances in nuclear-based hydrogen production and the thermochemical Cu-Cl cycle," *International Journal of Hydrogen Energy*, vol. 34, no. 7, 2009.
- [3] A. Farsi, "Development and modeling of a lab-scale integrated copper-chlorine cycle for hydrogen production," 2020.
- [4] L. C. Brown *et al.*, "High efficiency generation of hydrogen fuels using nuclear power," *Nuclear energy research initiative program U.S. department of energy*, 2003.

- [5] B. W. Mcquillan *et al.*, “High efficiency generation of hydrogen fuels using solar thermal-chemical splitting of water (Solar thermo-chemical splitting for H₂),” 2010.
- [6] M. A. Lewis, and J. G. Masin, “The evaluation of alternative thermochemical cycles - Part II: the down selection process, *International journal of hydrogen energy*”, vol. 34, pp. 4125 - 4135, 2009.
- [7] S. Kubo *et al.*, “A pilot test plan of the thermochemical water-splitting iodine- sulfur process,” *Nuclear engineering and design*, vol. 233, no. 1 - 3, pp. 355 - 362, 2004.
- [8] C. Sattler, M. Roeb, C. Agrafiotis, and D. Thomey, “Solar hydrogen production via sulphur based thermochemical water-splitting,” *Solar energy*, vol. 156, pp. 30 - 47, 2017.
- [9] Y. Shindo, N. Ito, K. Haraya, T. Hakuta, and H. Yoshitome, “Thermal efficiency of the magnesium-iodine cycle for thermochemical hydrogen production,” *International journal of hydrogen energy*, vol. 8, no. 7, pp. 509 - 513, 1983.
- [10] F. Lemont, “Promising optimization of the CeO₂/CeCl₃ cycle by reductive dissolution of cerium (IV) oxide,” *International journal of hydrogen energy*, vol. 33, no. 24, pp. 7355 - 7360, 2008.
- [11] F. Safari, and I. Dincer, “A study on the Fe – Cl thermochemical water splitting cycle for hydrogen production,” *International journal of hydrogen energy*, vol. 45, no. 38, pp. 18867 - 18875, 2020.
- [12] *Naterer et al.*, “Canada’s program on nuclear hydrogen production and the Cu-Cl thermochemical cycle,” *International journal of hydrogen energy*, vol. 35, pp. 10905-10926, 2010.
- [13] K. Pope, “Multiphase flow and chemical reactor thermodynamics for hydrolysis and thermochemical hydrogen production,” 2012.
- [14] M. Al-Zareer, I. Dincer, and M. A. Rosen, “Development and assessment of a novel integrated nuclear plant for electricity and hydrogen production,” *Energy conversion and management*, vol. 134, pp. 221 - 234, 2017.

- [15] A. Farsi, I. Dincer, and G. F. Naterer, "Review and evaluation of clean hydrogen production by the copper–chlorine thermochemical cycle," *Journal of cleaner production*, vol. 276, p. 123833, 2020.
- [16] M. S. Ferrandon et al., "Hydrogen production by the Cu-Cl thermochemical cycle: Investigation of the key step of hydrolysing CuCl_2 to Cu_2OCl_2 and HCl using a spray reactor," *International journal of hydrogen energy*, vol. 35, no. 3, pp. 992 - 1000, 2010.
- [17] A. Farsi, Ö. Kayhan, C. Zamfirescu, I. Dincer, and G. F. Naterer, "Kinetic and hydrodynamic analyses of chemically reacting gas-particle flow in cupric chloride hydrolysis for the Cu-Cl cycle," *International journal of hydrogen energy*, vol. 44, no. 49, pp. 26783 - 26793, 2019.
- [18] V. N. Daggupati, G. F. Naterer, K. S. Gabriel, R. J. Gravelsins, and Z. L. Wang, "Equilibrium conversion in Cu-Cl cycle multiphase processes of hydrogen production," *Thermochemical acta*, vol. 496, no. 1 - 2, pp. 117 - 123, 2009.
- [19] M. F. Orhan, I. Dinçer, and M. A. Rosen, "Efficiency comparison of various design schemes for copper-chlorine (Cu-Cl) hydrogen production processes using Aspen Plus software," *Energy conversion and management*, vol. 63, pp. 70 - 86, 2012.
- [20] A. Ozbilen, I. Dincer, and M. A. Rosen, "Environmental evaluation of hydrogen production via thermochemical water splitting using the Cu-Cl Cycle: A parametric study," *International journal of hydrogen energy*, vol. 36, no. 16, pp. 9514 - 9528, 2011.
- [21] G. F. Naterer, S. Suppiah, L. Stolberg, M. Lewis, Z. Wang, M. A. Rosen, I. Dincer, K. Gabriel, A. Odukoya, E. Secnik., E. B. Easton, V. Papangelakis, "Progress in Thermochemical Hydrogen Production with the Copper-Chlorine Cycle," *International journal of hydrogen energy*, vol. 40, no. 19, pp. 6283 - 6295, May, 2015.

- [22] G. F. Naterer, S. Suppiah, M. A. Rosen, K. Gabriel, I. Dincer, O. Jianu, Z. Wang, E. B. Easton, B. M. Ikeda, G. Rizvi, I. Piore, K. Pope, J. Mostaghimi, and S. Lvov “Progress in thermochemical water splitting with the Cu-Cl cycle for hydrogen production,”
- [23] Naterer et al, “Canada’s program on nuclear hydrogen production and the Cu-Cl thermochemical cycle,” *International journal of hydrogen energy*, no. 35, pp. 10905-10926, 2010.
- [24] M. S. Ferrandon et al., “Hydrogen production by the Cu-Cl thermochemical cycle: Investigation of the key step of hydrolysing CuCl_2 to Cu_2OCl_2 and HCl using a spray reactor,” *International journal of hydrogen energy*, vol. 35, no. 3, pp. 992 - 1000, 2010.
- [25] M. A. Lewis, J. G. Masin, P. A. O’Hare, “Evaluation of alternative thermochemical cycles, Part I: the methodology,” *International journal of hydrogen energy*, vol. 34, 4115 - 4124, 2009.
- [26] M. S. Ferrandon, M. A. Lewis, F. Alvarez, and E. Shafirovich, “Hydrolysis of CuCl_2 in the Cu-Cl thermochemical cycle for hydrogen production: Experimental studies using a spray reactor with an ultrasonic atomizer,” *International journal of hydrogen energy*, vol. 35, no. 5, pp. 1895 - 1904, 2010.
- [27] A. Farsi, Ö. Kayhan, C. Zamfirescu, I. Dincer, and G. F. Naterer, “Kinetic and hydrodynamic analyses of chemically reacting gas-particle flow in cupric chloride hydrolysis for the Cu-Cl cycle,” *International journal of hydrogen energy*, vol. 44, no. 49, pp. 26783 - 26793, 2019.
- [28] W. J. Smith, “Effect of gas radiation in the boundary layer on aerodynamic heat transfer,” *Journal of the aeronautical sciences*, vol. 20, pp. 579 - 580, 1952.
- [29] R. Viskanta, and R. J. Grosh, "Boundary layer in thermal radiation absorbing and emitting media," *International journal of heat and mass transfer*, vol. 5, no. 9, pp. 795-806, 1962.
- [30] J. T. Howe, “Radiation shielding of the stagnation region of an opaque gas,” NASA technical note D-329, 1960.

- [31] L. P. Kadanoff, "Radiative transport within an abating body," *Transactions of ASME journal of heat transfer*, vol. C83, pp. 215 - 225, 1961.
- [32] R. Bataller, "Radiation effects in Blasius flow," *Applied mathematics and computation*, vol. 198, no. 1, pp. 333 - 338, 2008.
- [33] B. L. Kuo, "Heat transfer analysis for the Falkner-Skan wedge flow by the differential transformation method," *International journal of heat and mass transfer*, vol. 48, no. 23 - 24, pp. 5036 - 5046, 2005.
- [34] A. J. Chamkha and J. Peddieson Jr, "Boundary layer flow of a particulate suspension past a flat plate," *International journal of multiphase flow*, vol. 17, pp. 805 - 808, 1991.
- [35] S. K. Mishra, and P. K. Tripathy, "Numerical investigation of free and forced convection two-phase flow over a wedge," *AMSE: Journal of thermal science and engineering applications*, vol. 82, pp. 92, 2013.
- [36] M. Ferdows, and M. Q. Al-Mdallal, "Effects of Order of Chemical Reaction on a Boundary Layer Flow with Heat and Mass Transfer Over a Linearly Stretching Sheet," *American journal of fluid dynamics*, vol. 2, no. 6, pp. 89-94, 2013.
- [37] M. Hussain, Q. A. Ranjha, M. S. Anwar, S. Jahan, and A. Ali, "Eyring-Powell model flow near a convectively heated porous wedge with chemical reaction effects," *Journal of the Taiwan institute of chemical engineers*, vol. 139, 2022.
- [38] O. D. Makinde, "Similarity solution for natural convection from a moving vertical plate with internal heat generation and a convective boundary condition," *Thermal science*, vol. 15, 2011.
- [39] L. J. Crane, "Flow past a stretching plate," *ZAMP*, vol. 21, pp. 645-647, 1970.
- [40] E. M. A. Elbashbeshy, "Heat transfer over a stretching surface with variable heat flux," *Journal of physics D: applied physics*, vol. 31, pp. 1951-1955, 1998.

- [41] M. S. Abel, and N. Mahesha, "Heat transfer in MHD viscoelastic fluid flow over a stretching sheet with variable thermal conductivity, non-uniform heat source and radiation," *Applied mathematical modelling*, vol. 32, pp. 1965 - 1983, 2008.
- [42] R. M. Kasmani, S. Sivasankaran, M. Bhuvaneshwari, and Z. Siri, "Effect of chemical reaction on convective heat transfer of boundary layer flow in nanofluid over a wedge with heat generation / absorption and suction," *Journal of applied fluid mechanics*, vol. 9, no. 1, pp. 379 - 388, 2016.
- [43] E. K. Luckins, J. M. Oliver, C. P. Please, B. M. Sloman, and R. A. Van Gorder, "Modelling and analysis of an endothermic reacting counter-current flow," *Journal of fluid mechanics*, pp. 947 - 949, 2022.
- [44] A. Pantokratoras, "The Falkner–Skan flow with constant wall temperature and variable viscosity," *International journal of thermophysics*, vol. 45, pp. 378 - 389, 2006.
- [45] S. K. Mishra, and P. K. Tripathy, "Mathematical and numerical modeling of two-phase flow and heat transfer using non-uniform grid," *Far East journal of applied mathematics*, vol. 54, pp. 107-126, 2011.
- [46] H. Xu, "A homogeneous-heterogeneous reaction model for heat fluid flow in the stagnation region of a plane surface," *International communications in heat and mass transfer*, vol. 87, pp. 112 - 117, 2017.
- [47] G. K. Ramesh, and B. J. Gireesha, "Flow over a stretching sheet in a dusty fluid with radiation effect," *Journal of heat transfer*, vol. 135, pp. 1027021 - 1027026, 2013.
- [48] B. J. Gireesha, S. Manjunatha, and C. S. Bagewadi, "Effect of radiation on boundary layer flow and heat transfer over a stretching sheet in the presence of a free stream velocity," *Journal of Applied Fluid Mechanics*, vol. 7, pp. 15 - 24, 2014.

- [49] B. J. Gireesha, B. Mahanthesh, R. S. R. Gorla, and K. L. Krupalakshmi, "Mixed convection two-phase flow of Maxwell fluid under the influence of non-linear thermal radiation, non-uniform heat source / sink and fluid-particle suspension," *Ain Shams Engineering Journal*, vol. 9, pp. 735 - 746, 2018.
- [50] Y. M. Sohn, S. W. Baek, and D. Y. Kim, "Thermophoresis of particles in gas-particle two-phase flow with radiation effect," *Numerical Heat Transfer, Part A* 41, pp. 165 - 181, 2002.

Chapter 3 – Radiation Effects on a Chemically Reacting Flow with Hydrolysis

A section of this chapter has been published as: S. Rimal, K. Pope, G. F. Naterer, K. A. Hawboldt. ‘Effects of Radiation on a Chemically Reacting Flow with Hydrolysis’ at the Proceedings of the Canadian Society for Mechanical Engineering International Congress, 2023, and ‘Semi-Analytical Model of Radiative Heat Transfer and Chemical Reactions in a Boundary Layer’ at the AIAA Science and Technology Forum and Exposition, 2024. The author of this thesis, Samita Rimal, was primary author of the papers and conducted all numerical modeling and analysis. Dr. Kevin Pope and Dr. Greg F. Naterer served as the principal supervisors, offering technical guidance, supervision, analytical support, and editing and are co-authors of the papers. Furthermore, Dr. Kelly A. Hawboldt provided technical guidance, analytical support, and contributed to the editing and is a co-author of the papers.

Abstract

This study focuses on modeling heat and fluid flow with a chemical reaction in the hydrolysis step of the Copper-Chlorine (Cu-Cl) cycle. A semi-analytical model is presented to investigate the effects of thermal radiation on the laminar boundary layer in the presence of a chemical reaction during the process. There have been several past studies on the heat and mass transfer of hydrolysis reactors to better understand their relative roles and optimize the overall cycle efficiency. There is limited work in examination of the effect of radiation during the process. The model accounts for changes during the process including variations in the specific heat and chemical reaction constant. A similarity transformation is used to convert the governing partial differential equations to ordinary differential equations. The numerical method of solution is based on a shooting method with a Runge-Kutta iteration method. The Rosseland approximation is utilized to study thermal

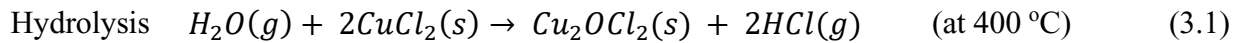
radiation and numerical simulations are conducted for cases with and without radiation. Past studies indicate that the presence of thermal radiation thickens the boundary layer and broadens the temperature distribution. This concept is studied and extended to the hydrolysis step of thermochemical hydrogen production in this chapter.

The model is first validated by a previously established system of equations and then extended to report the effects of radiation on the temperature and concentration gradients in the boundary layer during the hydrolysis process. Sensitivity analysis is performed to report the influence of radiation and chemical reaction parameters in detail. The thickness of the thermal boundary layer was observed to be increasing with the impact of higher radiation parameters. The importance of accounting for temperature dependency of the reaction rate constant in the boundary layer study was also noted. The result of this study provides useful data and trends to better understand the effects of radiation and chemical reactions on the boundary layer characteristics.

3.1 Introduction

There are numerous factors which influence the heat transfer processes in chemical reacting flows. Thermal radiation and the nature of the reaction, such as the number of reacting constituents, affect the flow characteristics. The reaction rate varies with concentration, temperature and pressure since the frequency of collisions among reactants increases at higher concentrations and temperatures. Radiative heat transfer increases the reaction rate at higher temperatures due to more energetic colliding particles with higher activation energies to initiate the chemical reactions. Also, the presence of a catalyst increases the rate of reaction since it provides an alternative reaction pathway at a lower activation energy. This chapter examines the various interactions between thermal radiation and chemical reactions in a thermally developing boundary layer flow.

Hydrolysis is a chemical reaction in which a molecule of water breaks one or more chemical bonds. Hydrolysis occurs in various engineering systems, for example, in thermochemical processes of hydrogen production [1, 2]. In the thermochemical copper-chlorine (Cu-Cl) cycle, a hydrolysis reaction occurs between high temperature steam and solid copper chloride as represented by Equation (3.1). The hydrolysis reaction is an endothermic non-catalytic gas-solid reaction at a temperature around 400 °C where CuCl₂ particles from the crystallization process are reacted with superheated steam to produce copper oxychloride solid (Cu₂OCl₂) and hydrogen chloride in gaseous form (HCl).



The overall reactant conversion rate in this reaction can be substantially affected by the mass and heat transfer rates [3]. The overall reactant conversion rates can be substantially affected by transport phenomena. The mass and/or heat transfer rates are influenced in the presence of chemical reaction processes [3]. The significance of thermal boundary-layers for two-dimensional steady and incompressible laminar flow past a plate, wedge or axisymmetric bodies have been examined previously [4 - 7]. Two-dimensional laminar boundary layer-flow and convective heat transfer have been studied by other investigators. However, studies of thermal radiation as an additional factor are limited [5, 6]. Thermal radiation affects heat transfer both directly and indirectly [5 - 7]. Radiative heat transfer can either be directly absorbed or emitted by a surface, altering the surface heat-transfer characteristics. Thermal radiation may be indirectly and partially absorbed in the boundary layer, impacting temperature distribution, and impacting the properties of convection and conduction [3]. Changes in temperature can impact temperature sensitive reactions (i.e. high activation energies).

A semi-analytical model of the hydrolysis reaction is discussed incorporating thermal radiation and utilizing a similarity transformation to numerically solve the governing equations. The numerical method employed is the Runge-Kutta shooting method in MATLAB. The effects of thermal radiation on the temperature distribution and heat transfer during the flow of a chemically reacting and absorbing / emitting medium is presented. The conservation of energy transforms into a nonlinear integrodifferential equation when energy transfer via radiation and convection is included. It is challenging to accurately analyze how a radiation field interacts with absorbing and emitting substances in the laminar boundary layer. The radiant-energy flux vector is approximated using the Rosseland approximation [5]. The method of solution is based on a similarity transformation utilizing the Runge-Kutta method together with a shooting method [8].

3.2 Mathematical Problem Formulation

When a fluid flows along any surface, a thin boundary layer is present where the transition from zero velocity at the wall reaches the full magnitude at some distance from the surface. In the boundary layer, the velocity gradient normal to the wall is $\partial u / \partial y$ and the shear stress $\tau = \mu(\partial u / \partial y)$ is large [9].

Similar to the momentum boundary layer, a thermal boundary layer exists when transfer of heat occurs in the fluid flow. It is known that when there is fluid flow with heat transfer and a chemical reaction, the overall reactant conversion may be significantly affected by transport phenomena or vice versa, when there are chemical reaction processes occurring in a regime, the overall mass and/or heat transfer rates can be significantly influenced [3].

The geometry of the problem, with an incompressible, two-dimensional, laminar boundary layer over a flat surface with momentum and thermal boundary layer is shown in Figure 3.1. The positive x-coordinate is measured along the surface while the y-axis is perpendicular to the surface.

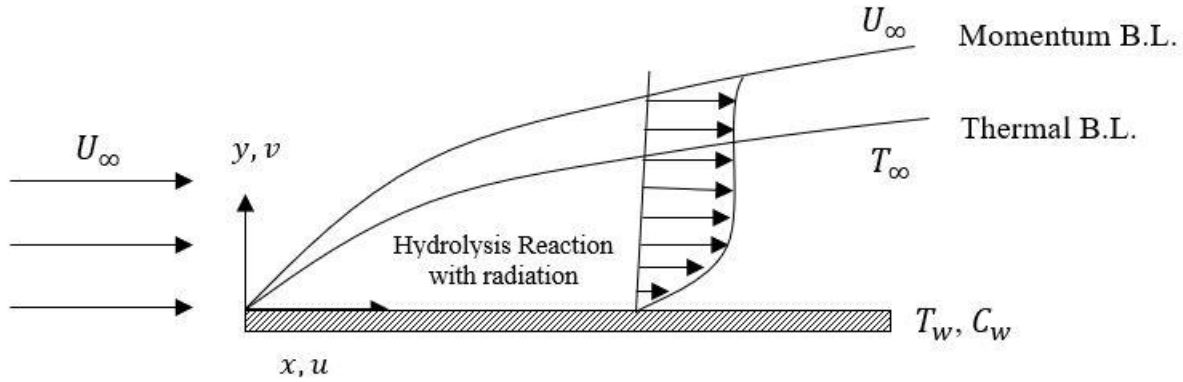


Figure 3.1 Geometry of the problem

The fluid flow along with a hydrolysis reaction is assumed to be an incompressible viscous flow over the flat plate. It is assumed that the flow in the laminar boundary layer is two-dimensional. The boundary layer equations are expressed as follows.

Mass Conservation

The continuity equation or conservation of mass expresses a balance between the mass entering and leaving a differential control volume per unit time, and the change in density [9]. For the case of steady, incompressible fluid, this leads to the following equation.

$$\frac{\partial u}{\partial x} + \frac{\partial v}{\partial y} = 0 \quad (3.2)$$

Conservation of momentum

The conservation of momentum or equation of motion is derived from Newton's Second Law, which states that the product of mass and acceleration is equal to the sum of the external forces acting on the body [9]. The momentum equation is a fundamental equation in fluid dynamics which describes the change in momentum of a fluid and plays a crucial role in understanding how velocity profiles change within the boundary layer. For this flow, momentum conservation in a cartesian coordinate system is expressed as:

$$u \frac{\partial u}{\partial x} + v \frac{\partial u}{\partial y} = \nu \frac{\partial}{\partial y} \left(\frac{\partial u}{\partial y} \right) \quad (3.3)$$

Conservation of energy

The energy conservation equation in a boundary layer describes the heat transfer and thermal distribution in a stagnation region of the surface. The governing equation for energy conservation considering the thermal radiation in the flow system can be expressed as:

$$\rho C_p \left(u \frac{\partial T}{\partial x} + v \frac{\partial T}{\partial y} \right) = k \frac{\partial^2 T}{\partial y^2} - \frac{\partial q_r}{\partial y} \quad (3.4)$$

where ρ is the density of the flow mixture, C_p is the specific capacity, and k and q_r represent thermal conductivity and radiative heat flux respectively.

Rosseland approximation is used to represent the radiant flux. The radiant-energy-flux (q_r) for a system close to thermodynamic equilibrium under this approximation can be written as [6, 10, 11]

$$q_r = - \frac{4\sigma}{3k^*} \frac{\partial T^4}{\partial y} \quad (3.5)$$

Where σ and k^* are the Stefan–Boltzmann constant and the mean absorption coefficient, respectively. To use the Rosseland approximation, it is assumed that the fractional temperature variation is modest across a distance of one mean free path and there is high absorption [11]. The temperature difference within the flow is expressed as a linear function of temperature. Hence, expanding T^4 in a Taylor series about T_∞ and neglecting higher-order terms, Equation (3.7) is reached. Rosseland’s approximation is developed in refs. [12, 13].

$$T^4 \cong 4T_\infty^3 T - 3T_\infty^4 \quad (3.6)$$

$$u \frac{\partial T}{\partial x} + v \frac{\partial T}{\partial y} = \left(\alpha + \frac{16\sigma T_\infty}{3\rho C_p k^*} \right) \frac{\partial^2 T}{\partial y^2} \quad (3.7)$$

Here if we consider $N_R = \frac{k k^*}{4\sigma T_\infty^3}$ as the radiation parameter with $k_0 = \frac{3N_R}{3N_R+4}$, Equation (3.7) can be represented as [6]. Higher values of the radiation parameter (N_R) results in a reduction in the impact of thermal radiation given by a non-radiating case where $k_0 = 1$. The equation (3.8) reduces to the energy conservation equation for simple Blasius flow when thermal radiation is absent at $k_0 = 1$.

$$u \frac{\partial T}{\partial x} + v \frac{\partial T}{\partial y} = \frac{\alpha}{k_0} \frac{\partial^2 T}{\partial y^2} \quad (3.8)$$

where α is the thermal diffusivity.

Species Conservation

The species conservation equation provides insight into how chemical species are transported and react within the boundary layer. The equation describes how a constituent is transported by the flow, diffuses through the fluid, and undergoes a chemical reaction depending on the species concentration [3, 8, 14]. Considering species diffusion in the y-direction and reaction rate control by a chemical reaction, the species conservation equation is expressed as:

$$u \frac{\partial C}{\partial x} + v \frac{\partial C}{\partial y} = D \frac{\partial^2 C}{\partial y^2} - bk_1 C_\infty C \quad (3.9)$$

where b is the stoichiometric reaction coefficient, k_1 is the chemical reaction constant, C_∞ is steam concentration, C is the solid particle concentration and D is the effective diffusion coefficient.

The associated boundary conditions for this system of equations are given as follows:

$$\left. \begin{aligned} u = v = 0, \quad T = T_w, \quad C = C_w \text{ at } y = 0 \\ u = U_\infty, \quad T = T_\infty, \quad C = C_\infty \text{ at } y \rightarrow \infty \end{aligned} \right\} \quad (3.10)$$

Where T_w is the constant temperature of the wall, T_∞ is a constant temperature of the ambient fluid ($T_\infty > T_w$) and U_∞ is a constant free stream velocity and ($C_\infty > C_w$).

3.3 Modeling

3.3.1 Similarity Transformation

The solution of the boundary layer equations utilizing similarity solutions has been extensively reported by Schlichting [9]. Similarity transformations are used to deal with the problem equations for non-dimensionality. In cases when a similarity solution exists, the system of partial differential equations can be reduced to a system involving ordinary differential equations which constitute a mathematical simplification of the problem. A similarity transformation is used to solve the system of governing PDEs represented by Equations (3.2) to (3.9).

Similarity variables are introduced by defining a stream function $\psi(x, y)$ as a function of the velocity component in x-direction and y-direction.

$$u = \frac{\partial \psi}{\partial y} \quad (3.11)$$

$$v = -\frac{\partial\psi}{\partial x} \quad (3.12)$$

The similarity variable along with dimensionless terms are introduced in Equations (3.11) to (3.15). Here η is the similarity variable, f is the dimensionless stream function, θ is the dimensionless temperature, and ϕ is the dimensionless concentration.

$$\eta = y \sqrt{\frac{U_\infty}{\nu x}} \quad (3.11)$$

$$f'(\eta) = \frac{u}{U_\infty} \quad (3.12)$$

$$\psi = \sqrt{\nu U_\infty x} f(\eta) \quad (3.13)$$

$$\theta = \frac{T - T_\infty}{T_w - T_\infty} \quad (3.14)$$

$$\phi = \frac{C - C_\infty}{C_w - C_\infty} \quad (3.15)$$

3.3.2 Governing ODEs

The partial differential equations (3.3), (3.7) and (3.9) and the associated boundary conditions (3.10) can be transformed to a set of ordinary differential equations by substituting respective similarity variables. The following set of reduced dimensionless equations and associated boundary conditions are obtained after the transformation:

$$2f''' + ff'' = 0 \quad (3.16)$$

$$\theta'' + \frac{Prk_o}{2} f\theta' = 0 \quad (3.17)$$

$$\phi'' - Sc \left[2K\phi - \frac{\phi'f}{2} \right] = 0 \quad (3.18)$$

where Pr is the Prandtl number and $f'(\eta) = \frac{u}{U_\infty}$. The dimensionless temperature and concentration are represented by θ and ϕ respectively. The Schmidt number is $Sc = \frac{\nu}{D}$ and chemical reaction parameter is $K = \frac{k_1 C_\infty x}{U_\infty}$ with $Kr = \frac{C_\infty x}{U_\infty}$. The boundary conditions reduce to:

$$\left. \begin{aligned} f = f' = 0, \theta(0) = 1, \phi(0) = 1 \text{ as } \eta = 0 \\ f'(\infty) = 1, \theta(\infty) = 0, \phi(\infty) = 0 \text{ as } \eta = \infty \end{aligned} \right\} \quad (3.19)$$

3.4 Results and Discussion

3.4.1 Results

The set of equations were solved numerically with $\Delta\eta = 0.01$ and a residual error less than 10^{-5} for all cases employing a fourth order shooting method. Numerical solutions are presented for a Prandtl number of 1 as selected for steam, Schmidt number of 0.62 for water vapor and chemical reaction parameter $K = 1$.

The parameters for the present study are the radiation parameter N_R and chemical reaction parameter, K . Since the flow problem is uncoupled from the thermal problem, changes in the values of N_R will not affect the fluid velocity and is not studied in this chapter. Hence, the function $f(\eta)$ and its derivatives are identical, and the physical quantities of interest are the temperature profile $\theta'(0)$ and the concentration profile $\phi'(0)$.

Figures 3.2 and 3.3 demonstrate the temperature profile and temperature gradients as a function of the similarity variable, across the boundary layer. The temperature profiles for the case without radiation, $k_0 = 1$ and for the cases with the thermal radiation parameter, $N_R = 0.3, 0.7$ and 1, are considered. The value of $N_R = 0.3$ represents the temperature profile observed when the

thermal radiation effect is maximum. Then $N_R = 1$ is the case when the magnitude of radiation is the same order of magnitude as conduction and $k_0 = 1$ occurs when thermal radiation is absent. The effect of radiation is to thicken the thermal boundary layer similar to the effect of lowering the Prandtl number. From the wall to the free stream, the dimensionless temperature monotonically varies throughout the boundary layer. The cases with radiation are represented by $N_R = 0.3, 0.7$ and 1 in increasing order of the radiation term. Compared to the deviation between $N_R = 0.3$ and $k_0 = 1$, the deviation of the $N_R = 1$ trends with the $k_0 = 1$ plot is minimal. This characterizes the effects of thermal radiation to widen the temperature distribution.

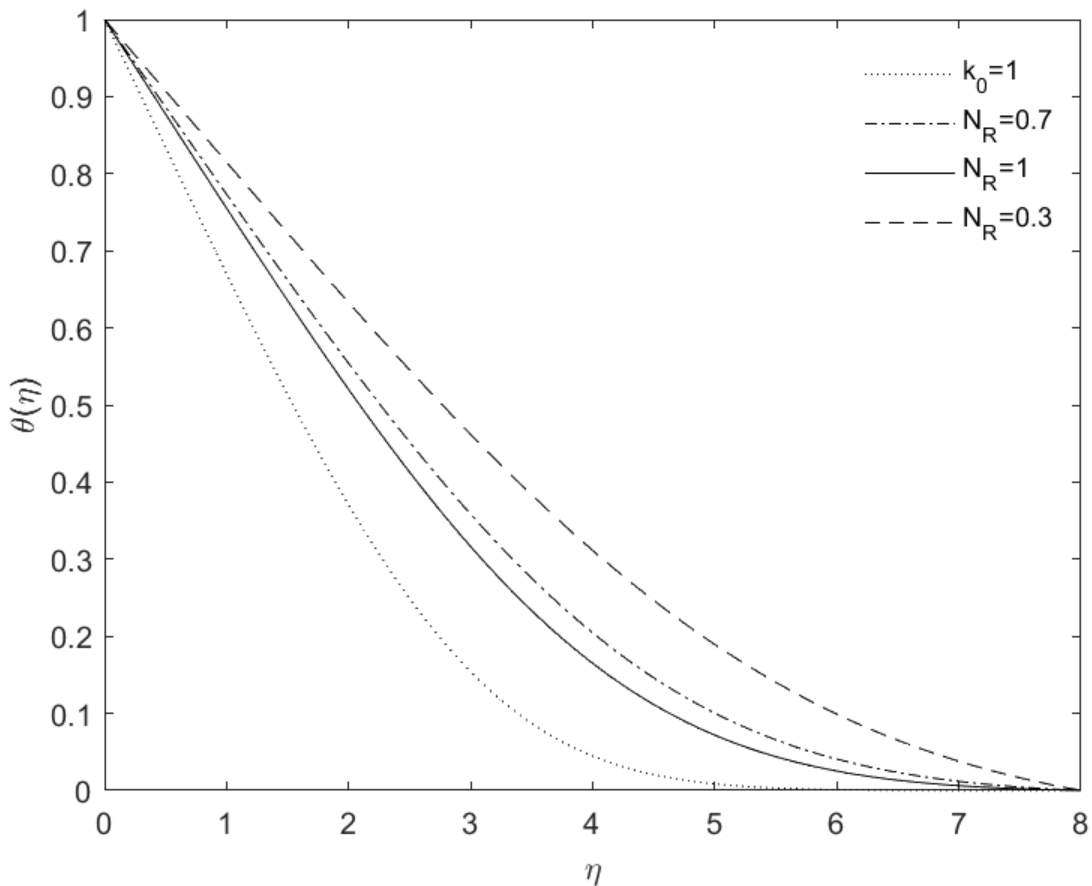


Figure 3.2 Temperature distribution across boundary layer as a function of η for cases with radiation ($N_R = 0.3, 0.7$ and 1) and without radiation ($k_0 = 1$)

Figure 3.3 shows the variation of heat transfer across the boundary layer in terms of a temperature gradient and is also comparable to the boundary layer temperature gradient study by Viskanta and Grosh [5]. It is noted that the temperature gradient is a maximum at some point away from the wall. This trend is observed due to the non-linear dependence of the radiant energy flux on the temperature as represented by the energy equation (3.8). The effect of radiation is to increase the temperature gradient as compared to the case without radiation. Near the wall or boundary, a steeper gradient is observed in the presence and absence of radiation, indicating an increase of heat transfer.

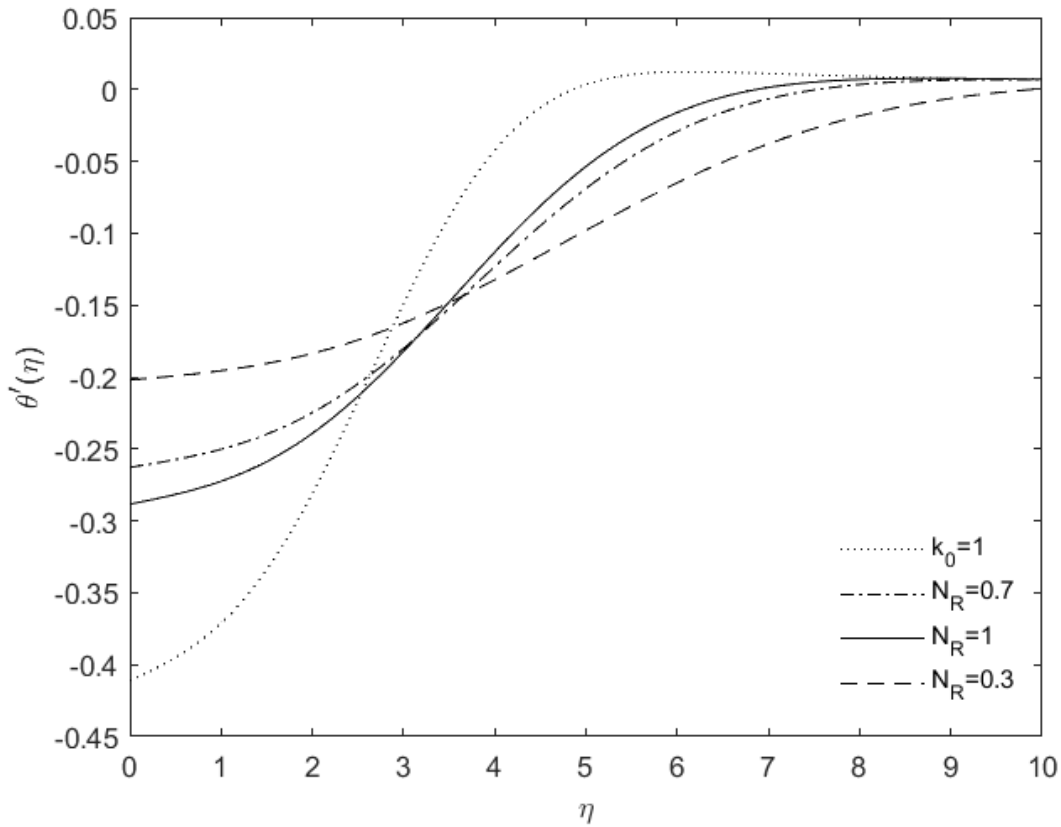


Figure 3.3 Temperature gradient across boundary layer as a function of η for cases with radiation ($N_R = 0.3, 0.7$ and 1) and without radiation ($k_0 = 1$)

Figure 3.4 illustrates that when a constant value of the chemical reaction constant is considered, the results converge faster indicating a higher extent of conversion. The dash-dotted line is the actual representation when accounting for the variation in the chemical reaction constant, K due to the temperature dependency of the hydrolysis reaction rate constant in the boundary layer. This study underscores the significance of integrating temperature-dependent reaction rate constants and their impact on the concentration gradient within the boundary layer and is discussed in detail in the next chapter.

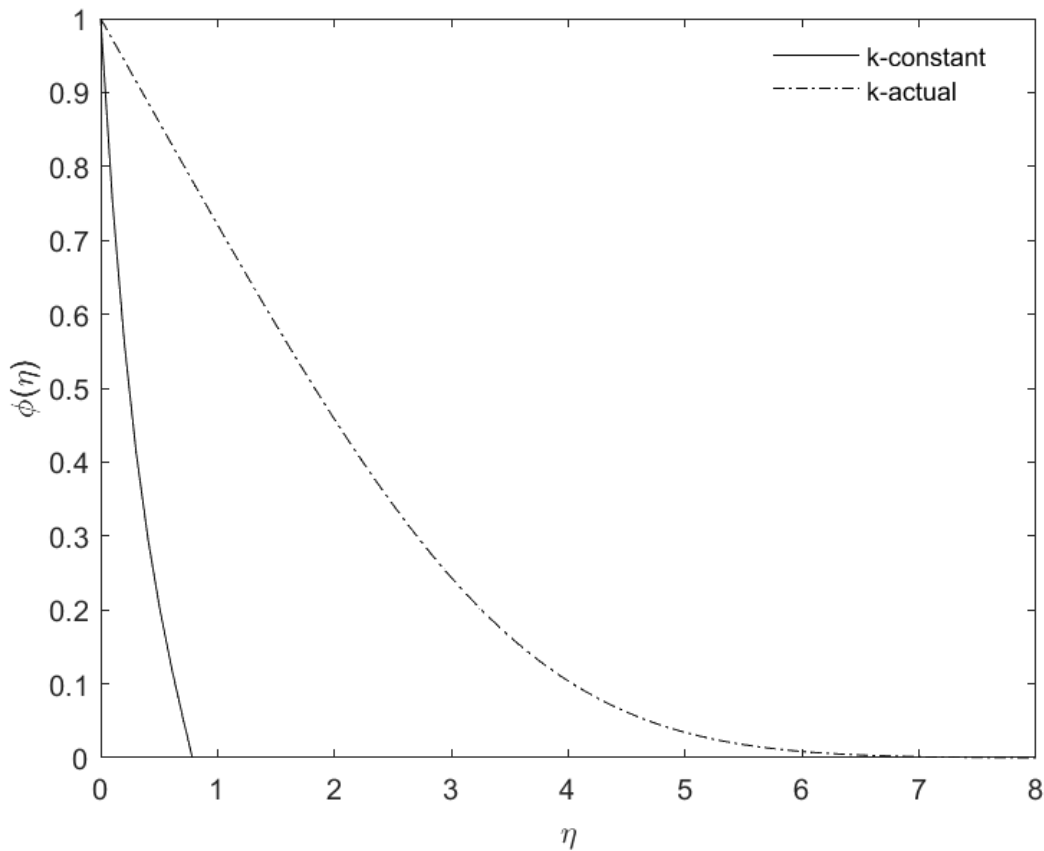


Figure 3.4 Concentration profile as a function of η for radiation case, $N_R = 0.7$

Table 3.1 summarizes the calculated values of the rate of heat transfer $\theta'(0)$ and the rate of mass transfer $\phi'(0)$ with $Pr = 1$, $Sc = 0.62$ for $k_0 = 1$ and cases with radiation, $N_R = 0.3, 0.7$ and 1 . It is observed that the effect of radiation is to increase the heat transfer rate.

Table 3.1 Values of the rate of heat transfer $\theta'(0)$ and the rate of mass transfer $\phi'(0)$

η	$-\theta'(0)$				$-\phi'(0)$			
	$k_0 = 1$	$N_R = 1$	$N_R = 0.7$	$N_R = 0.3$	$k_0 = 1$	$N_R = 1$	$N_R = 0.7$	$N_R = 0.3$
0	0.3321	0.2456	0.2273	0.1894	0.8074	0.8074	0.8074	0.8074
1	0.3226	0.2426	0.2251	0.1855	0.3718	0.3718	0.3718	0.3718
2	0.2645	0.2228	0.2102	0.1732	0.1652	0.1652	0.1652	0.1652
3	0.1571	0.1782	0.1756	0.1616	0.0657	0.0657	0.0657	0.0657
4	0.0605	0.1184	0.1265	0.1210	0.0219	0.0219	0.0219	0.0219
5	0.0143	0.0638	0.0770	0.0962	0.0059	0.0059	0.0059	0.0059
6	0.0025	0.0304	0.0425	0.0631	0.0014	0.0017	0.0016	0.0017
7	0.0002	0.0108	0.0185	0.0362	0.0002	0.0002	0.0002	0.0002
8	0.0000	0.0031	0.0067	0.0171	0.0000	0.0000	0.0000	0.0000

3.4.2 Validation

Equations (3.16) and (3.17) also represent the governing system of equations utilized to study radiation effects in the boundary layer in the Blasius flow [6]. The existing numerical technique was validated with the study of radiation effects in the Blasius flow by Bataller [6] and presented in Figure (3.5). Numerical solutions were obtained using a fourth-order shooting method, with a step size ($\Delta\eta$) of 0.01 and a residual error below 10^{-5} for Prandtl number of 0.7, 5 and 10. Through

this analysis, it was established that the fourth order Runge-Kutta method utilized for this model and throughout the thesis is accurate and effective.

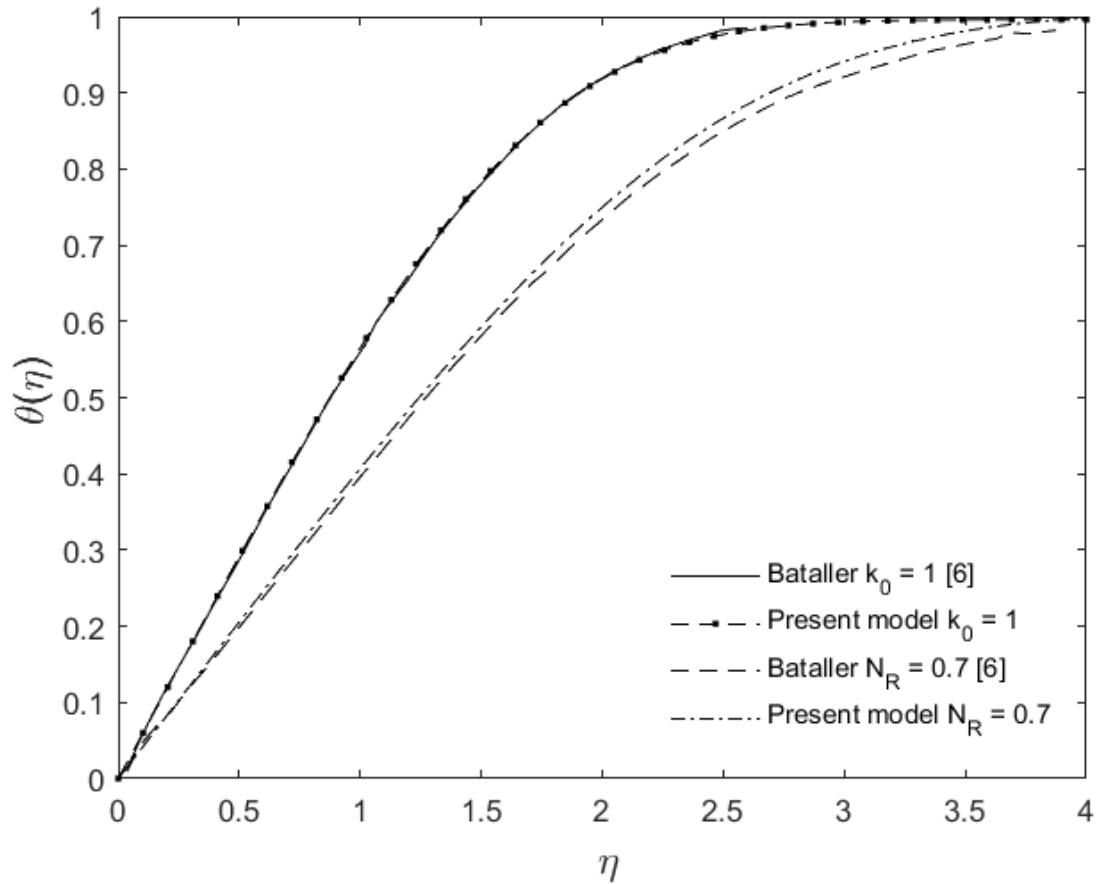


Figure 3.5 Comparison of numerical method with Bataller [6]

Table 3.2 provides a comprehensive comparison of dimensionless temperature gradients denoted as $\theta'(0)$ derived from the research conducted by Bataller [6] with the outcomes of the current study. Prandtl numbers of 0.7, 5 and 10 are selected for a case without radiation ($k_0 = 1$) and two radiation cases ($N_R = 0.7$ and 1). The close agreement among the findings underscores the robustness and reliability of the analysis, demonstrating that the conclusions hold true for a wide range of Prandtl numbers and radiation conditions.

Table 3.2 Validation of numerical model

Pr	N_R	k_0	$\theta'(0)$	$\theta'(0)$ [6]
0.7	–	1	0.3242	0.29268
10	–	1	0.7427	0.72814
5	0.7	–	0.4120	0.40106
5	1	–	0.4416	0.43240
5	–	1	0.5860	0.57643

3.5 Conclusions

This chapter analyzed laminar boundary layer flow over a surface in the presence of a chemical reaction and thermal radiation. With the use of a similarity transformation, the partial differential equations were transformed to ordinary differential equations and then solved with a fourth order Runge-Kutta shooting method. Numerical solutions were obtained for temperature and concentration profiles, and temperature gradients across the boundary layer. Three cases for radiation, $N_R = 0.3, 0.7$ and 1 , were studied and compared with a case without radiation $k_0 = 1$. The numerical results showed the effectiveness of the uncoupled flow equation with the energy equation to predict the temperature and concentration values.

In a two-dimensional laminar boundary-layer flow, heat transfer studies with convection have been studied, however, cases with thermal radiation have not been previously examined in depth. A detailed analysis to evaluate the effects of transport phenomena in the presence of radiation effects was presented in this chapter. Through the investigation of the temperature profile, a significant role of thermal radiation in the boundary layer of the flow was observed – an increased radiative parameter caused an increase in the thickness of boundary layer. The thermal boundary layer

thickness is increased with the impact of thermal radiation and was noted that the temperature gradient is a maximum at a point away from the wall.

Computation of the temperature dependent chemical reaction constant and a constant reaction rate demonstrated the significance of accounting for the temperature dependence of the chemical reaction rate constant with temperature ranges in the reactor. Overall, these results have useful potential for conversion improvement within the hydrolysis process by better understanding the boundary layer heat and mass transfer. The findings also highlighted a significant role in the concentration profile which is explored in more detail in the next chapter.

References

[1] M. A. Lewis, M. M. Serban, and J. K. Basco, "Nuclear production of hydrogen, second information exchange meeting Argonne," *Argonne, Illinois: Argonne National Laboratory*, pp. 145 - 156, 2003.

[2] G. F. Naterer, I. Dincer, and C. Zamfirescu, "Hydrogen production from nuclear energy," Springer, New York, NY, 2013.

[3] H. Xu, "A homogeneous-heterogeneous reaction model for heat fluid flow in the stagnation region of a plane surface," *International communications in heat and mass transfer*, vol. 87, pp. 112 - 117, 2017.

[4] B. L. Kuo, "Heat transfer analysis for the Falkner-Skan wedge flow by the differential transformation method," *International journal of heat and mass transfer*, vol. 48, no. 23-24, pp. 5036-5046, 2005.

[5] R. Viskanta, and R. J. Grosh, "Boundary layer in thermal radiation absorbing and emitting media," *International journal of heat and mass transfer*, vol. 5, no. 9, pp. 795-806, 1962.

- [6] R. Bataller, "Radiation effects in Blasius flow," *Applied Mathematics and Computation*, vol. 198, no. 1, pp. 333-338, 2008.
- [7] A. Pantokratoras, and T. Fang, "Blasius flow with non-linear Rosseland thermal radiation," *Meccanica*, vol. 49, no. 6, 2014.
- [8] M. Ferdows, and M. Q. Al-Mdallal, "Effects of order of chemical reaction on a boundary layer flow with heat and mass transfer over a linearly stretching sheet," *American journal of fluid dynamics*, vol. 2, no. 6, pp. 89 - 94, 2013.
- [9] H. Schlichting, "Boundary layer theory," 2nd edition, Pergamon press, New York, 1955.
- [10] A. Raptis, C. Perdikis, and H. S. Takhar, "Effect of thermal radiation on MHD flow," *Applied mathematics and computation*, vol. 153, no. 3, pp. 645 - 649, 2004.
- [11] S. Rosseland, "Astrophysics on an atomic theoretical basis," vol. 42, Springer, Berlin, 1931.
- [12] R. Viskanta, "Heat transfer in thermal radiation absorbing and scattering media," ANL-6170, 1960.
- [13] G. F. Naterer, "Advanced heat transfer," 3rd edition, CRC Press, Boca Raton, FL, 2021.
- [14] V. N. Daggupati, G. F. Naterer, and K. S. Gabriel, "Diffusion of gaseous products through a particle surface layer in a fluidized bed reactor," *International journal of heat and mass transfer*, vol. 53, no. 11-12, pp. 2449-2458, 2010.

Chapter 4 – Solid-Gas Flow with Variable Thermophysical Properties

This chapter has been submitted to a journal for consideration of publication with Samita Rimal, Dr. Kevin Pope, Dr. Greg F. Naterer and Dr. Kelly A. Hawboldt as the co-authors. The author of this thesis, Samita Rimal, was first author of the paper and conducted all numerical modeling and analysis. Dr. Kevin Pope and Dr. Greg F. Naterer served as the principal supervisors, offering technical guidance, supervision, analytical support, and editing and are co-authors of the paper. Furthermore, Dr. Kelly A. Hawboldt provided technical guidance, analytical support, and contributed to the editing and is a co-author of the paper.

Abstract

This chapter investigates the combined effects of radiative heat transfer and chemical reactions on a participating gas-solid flow. In the hydrolysis reaction, a specific focus is placed on the influence of thermal radiation as characterized by parameters dependent on temperature. A semi-analytical framework is presented to investigate the effects of temperature dependent thermophysical properties including thermal conductivity, specific heat and dynamic viscosity. By employing similarity transformations, the governing equations are solved to obtain similarity solutions using a fourth-order Runge-Kutta method. Initially, the model undergoes validation by a previously established benchmark problem and is expanded further to investigate the effect of varying parameters. Deviations in the Prandtl and Schmidt numbers within the boundary layer are also presented for thermal conductivity and dynamic viscosity varying with temperature. Radiation significantly influences the boundary layer flow. Higher radiation parameters and the presence of a chemical reaction led to an increase in the boundary layer thickness. Furthermore, it was also established that the effect of a chemical reaction on the thermal boundary layer is minimized in

the presence of radiation. The presence of solid particles is found to enhance the heat and mass transfer and affect the concentration profile. Examining the combined influence of varying thermophysical properties and thermal radiation reveals a decline in the chemical species concentration near the surface. This could be due to enhanced mass transfer, an increment in the reaction rate, or changes in fluid properties with temperature in promoting faster diffusion of species away from the boundary.

4.1 Introduction

Due of its extensive range of applications, researchers have investigated boundary layer heat transfer and fluid flow across surfaces. Understanding the heat and mass transfer in boundary layers is particularly significant in transport processes at solid surfaces [1]. There are several factors that influence the heat transfer in participating solid-gas flow with chemical reactions. Thermal radiation, temperature dependency of thermophysical properties, and the nature of the reaction, such as the reacting constituents and heat generation / absorption affect the flow characteristics.

Past studies of radiation in a boundary layer flow were reported by Smith [2]. The effects of thermal radiation on heat transfer in a medium that both absorbs and emits energy were reported by Viskanta and Grosh [3]. Howe [4] and Kadanoff [5], showed that thermal radiation has a potential to influence heat transfer through direct and indirect mechanisms. Within the boundary layer, thermal radiation might undergo partial absorption, resulting in changes to the temperature distribution and subsequent impacts on heat transfer [4,6].

Other studies [6-11] have analyzed various geometries and surfaces in terms of thermal radiation processes. Two-dimensional thermal boundary layers around a wedge, flat surface, or

axisymmetric body have been extensively examined [12-16]. The Blasius boundary layer describes a steady two-dimensional viscous flow near solid surfaces [17]. Bataller [6] reported the radiation effects in Blasius flow and discussed their significance at high operating temperatures. Other studies also discussed radiation effects in Magnetohydrodynamic (MHD) flows [18-20]. The fluid flow characteristics within the boundary layer over a wall or a stretching surface, both with and without thermal radiation, were well documented in previous studies [15, 21-24].

Past studies have also examined flow in the boundary layer under the influence of chemically reacting flows with, and, without, thermal radiation effects and using constant and/or variable thermophysical properties in the flow [16, 24-31]. Studies of the interaction of heat transfer with chemical processes often correspond to combustion and flames [32]. Previous studies have developed models for endothermic reacting flows in a counter-current configuration, including the significance of particles in the flow. This role affects the heat transfer and skin friction in proximity of the surface [29]. Investigations by Chamkha et al. [13], as well as Mishra and Tripathy [14, 33], highlighted both analytical and numerical solutions for flows involving multiple phases. They concluded that the presence of solid particles leads to significant changes in heat transfer as well as the shear stress on the wall surface. Similarly, in the presence of chemical reactions in the flow, overall conversion rate of reactants can be significantly influenced by the mass and heat transfer rates [34].

Hydrolysis involves a chemical reaction where the breaking of one or more chemical bonds by a water molecule occur. Hydrolysis occurs in various engineering systems, such as thermochemical processes of hydrogen production [27]. The hydrolysis process has a crucial role in the overall efficiency of the thermochemical Cu-Cl hydrogen production cycle. In the Cu-Cl cycle, a

hydrolysis reaction occurs between high temperature steam and solid copper chloride as follows [35].



The reaction rate changes as a result of changes in concentration, temperature, and pressure as higher concentrations and temperatures lead to an increased frequency of collisions between reactants. When radiative heat transfer is present, higher temperatures result in an increased reaction rate because the particles collide with greater energy and possess higher activation energies to initiate chemical reactions. Hydrolysis is a highly temperature sensitive endothermic reaction in the thermochemical copper-chlorine cycle [35-38]. Past study by Zamfirescu et al. [39] has reported the thermophysical properties of copper compounds within the Cu-Cl cycle. However, none of the studies examined the radiation effects when hydrolysis reaction occurs in the boundary layer flow with variable thermophysical properties. Also, there are few or no studies examining the collective effects of radiative heat transfer and chemical reactions incorporating temperature dependent thermophysical properties in hydrolysis. This section examines the various interactions between thermal radiation and an endothermic reaction under the conditions of temperature dependent thermophysical properties to examine the characteristics of heat and mass transfer occurring in the boundary layer flow.

In the analysis of the endothermic hydrolysis reaction, the model incorporates elements such as thermal radiation, temperature-dependent specific heat capacity, thermal conductivity, and viscosity. It employs a similarity transformation to solve the governing equation system. The solution method is a Runge-Kutta shooting technique using MATLAB. In-depth investigations are conducted to explore the impacts of thermal radiation on temperature distribution and heat transfer in the context of flowing through a chemically reacting medium that also absorbs/emits. Also,

effects of different thermophysical property changes are investigated for a range of temperatures. Numerical and analytical studies of fluid flow and transport phenomena are utilized to validate and improve the understanding of heat and mass transfer in the boundary layer.

4.2 Governing Equations

Fluid flow with a hydrolysis reaction is assumed to occur in an incompressible boundary layer flow over a flat surface. It is assumed that the flow is steady and fully developed. The flux of thermal radiation in the y-direction is negligible compared to the x-direction.

For numerical solutions, a shooting method is implemented, utilizing a Runge-Kutta iteration scheme. The examination of thermal radiation employs a Rosseland approximation. Numerical simulations are performed for scenarios with thermal radiation as well as without radiation. The mass and momentum conservation equations are presented below.

$$\frac{\partial u}{\partial x} + \frac{\partial v}{\partial y} = 0 \quad (4.2)$$

$$\rho \left(u \frac{\partial u}{\partial x} + v \frac{\partial u}{\partial y} \right) = \frac{\partial}{\partial y} \left(\mu \frac{\partial u}{\partial y} \right) \quad (4.3)$$

Equation (4.3) can also be represented as following

$$u \frac{\partial u}{\partial x} + v \frac{\partial u}{\partial y} = \nu \frac{\partial}{\partial y} \left(\frac{\partial u}{\partial y} \right) \quad (4.4)$$

The mixture density of the participating medium of gas-solid flow is defined as:

$$\rho = (1 - \omega)\rho_f + \omega\rho_s \quad (4.5)$$

where ω is the mass fraction of the solid particles and $(1 - \omega)$ represents the gas mass fraction.

The energy conservation equation for a participating gas-solid flow in a boundary layer describes the heat transfer and thermal distribution within the boundary layer as the gas and solid particles interact and flow over the solid surface. The energy equation incorporates a homogeneous reaction in the bulk fluid [34]. It is assumed that the chemical reaction requires heat absorption, and the effects of thermal expansion will be integrated into the boundary layer as a result of the reaction [34]. Assuming a rate controlled chemical reaction, Equation (4.6) is obtained [40].

$$\rho C_p \left(u \frac{\partial T}{\partial x} + v \frac{\partial T}{\partial y} \right) = \frac{\partial}{\partial y} \left(k \frac{\partial T}{\partial y} \right) - \frac{\partial q_r}{\partial y} - b k_1 C C_\infty \Delta H \quad (4.6)$$

Equation (4.6) is also be represented as following

$$\rho C_p \left(u \frac{\partial T}{\partial x} + v \frac{\partial T}{\partial y} \right) = k \frac{\partial^2 T}{\partial y^2} - \frac{\partial q_r}{\partial y} - b k_1 C C_\infty \Delta H \quad (4.7)$$

where ρ is total density of the solid-gas mixture, C_p is the specific heat of the mixture. k represents the thermal conductivity, b represents the stoichiometric reaction coefficient, C , C_∞ and ΔH represents the solid particle concentration, ambient steam concentration and the heat of reaction respectively. The heat of reaction (ΔH) is 117 kJ/mol [39]. The term on the left represents the advection of thermal energy by the fluid motion. The first term on the right describes how heat is transferred within the fluid through molecular diffusion, and $\frac{\partial q_r}{\partial y}$ accounts for radiative heat transfer in the y-direction while the last term represents the heat absorption due to chemical reactions.

The Rosseland approximation is applied to simplify the representation of the radiant flux. The radiant-energy-flux for a system close to thermodynamic equilibrium under the Rosseland approximation can be expressed as [6, 7, 41, 42].

$$q_r = -\frac{4\sigma}{3k^*} \frac{\partial T^4}{\partial y} \quad (4.8)$$

where k^* is the mean absorption coefficient and σ is the Stefan–Boltzmann constant.

To use the Rosseland approximation, the fractional temperature variation is assumed to be modest across a distance of one mean free path and there is high absorption. Additionally, assuming that the temperature variations in the flow allow the representation of the term T^4 as a linear function of temperature [6, 43], the expansion of T^4 using a Taylor series around T_∞ and disregarding the higher-order terms result in Equation (4.10). Rosseland's approximation is developed in [43, 44].

$$T^4 \cong 4T_\infty^3 T - 3T_\infty^4 \quad (4.9)$$

$$u \frac{\partial T}{\partial x} + v \frac{\partial T}{\partial y} = \left(\alpha + \frac{16\sigma T_\infty^3}{3\rho C_p k^*} \right) \frac{\partial^2 T}{\partial y^2} - bk_1 C C_\infty \Delta H \quad (4.10)$$

where $\alpha = \frac{k}{\rho C_p}$ is the thermal diffusivity.

Introducing $N_R = \frac{k k^*}{4\sigma T_\infty^3}$ as the radiation parameter [6], allows Equation (4.10) to be expressed as

$$u \frac{\partial T}{\partial x} + v \frac{\partial T}{\partial y} = \frac{\alpha}{k_0} \frac{\partial^2 T}{\partial y^2} - bk_1 C C_\infty \Delta H \quad (4.11)$$

where $k_0 = \frac{3N_R}{3N_R+4}$.

The properties of the mixture are represented by

$$\rho C_p = (1 - \omega)(\rho C_p)_f + \omega(\rho C_p)_s \quad (4.12)$$

The species conservation equation provides insight into how chemical species are transported and react within the boundary layer. The equation describes how a constituent is transported by the

flow, diffuses through the fluid, and undergoes a chemical reaction depending on the species concentration [15, 26, 34, 40]. Considering species diffusion in the y-direction and reaction rate control by a chemical reaction, the species conservation equation is expressed as

$$u \frac{\partial C}{\partial x} + v \frac{\partial C}{\partial y} = D \frac{\partial^2 C}{\partial y^2} - bk_1 C C_\infty \quad (4.13)$$

where C is the particle concentration, b represents the stoichiometric reaction coefficient, D is the effective diffusion coefficient, and k_1 is the chemical reaction constant. For a hydrolysis reaction operating at atmospheric pressure, steam mole fraction range of 0.4 - 0.9 and the temperature range of 275 °C to 375 °C, $k_1 = 2.4 \times 10^4 e^{(-44800/RT)}$ [36].

The temperature dependent thermal conductivity, viscosity, and specific heat for the fluid mixture is modelled by the Maxwell's power-law relation [26] and given by

$$\mu = \mu_\infty \left(\frac{T}{T_\infty} \right)^m \quad (4.14)$$

$$k = k_\infty \left(\frac{T}{T_\infty} \right)^n \quad (4.15)$$

$$C_p = C_{p,\infty} \left(\frac{T}{T_\infty} \right)^l \quad (4.16)$$

where μ_∞ , $C_{p,\infty}$, k_∞ are the dynamic viscosity, specific heat capacity, and thermal conductivity of the ambient fluid respectively and m , n and l are constants, commonly known as the viscosity constant, thermal conductivity constant and specific heat constant respectively.

The problem's boundary conditions are represented as follows

$$\left. \begin{aligned} u = v = 0, \quad T = T_w, \quad C = C_w \text{ at } y = 0 \\ u = U_\infty, \quad T = T_\infty, \quad C = C_\infty \text{ at } y \rightarrow \infty \end{aligned} \right\} \quad (4.17)$$

Similarity solutions of boundary layer problems have been extensively reported by Schlichting [17]. For two-dimensional inviscid flow, an alternative variable called the stream function, represented by $\psi(x, y)$ is adopted in order to simplify the equations in terms of this single variable. The energy conservation equation in a boundary-layer flow includes a nonlinear integrodifferential equation arising from the thermal radiation term.

As it is not feasible to obtain an analytical solution for this equation, a Rosseland approximation is employed. The governing equations are then reformulated into the following expressions, incorporating the terms involving similarity variables.

$$\eta = y \sqrt{\frac{U_\infty}{\nu x}} \quad (4.18)$$

$$\theta = \frac{T - T_\infty}{T_w - T_\infty} \quad (4.19)$$

$$\phi = \frac{C - C_\infty}{C_w - C_\infty} \quad (4.20)$$

$$\psi = \sqrt{\nu U_\infty x} f(\eta) \quad (4.21)$$

Here, η represents the similarity variable, θ is the dimensionless temperature, f is the dimensionless stream function, ϕ the dimensionless concentration, and ψ represents the stream function with the following expression:

$$u = \frac{\partial \psi}{\partial y} \quad (4.22)$$

$$v = -\frac{\partial \psi}{\partial x} \quad (4.23)$$

Substituting the similarity variables, the subsequent set of reduced equations and associated boundary conditions after the similarity transformation are obtained.

Using a similarity transformation, the Equations (4.14) to (4.16) become

$$\mu^* = \frac{\mu}{\mu_\infty} = (1 + \gamma\theta)^m \quad (4.24)$$

$$k^* = \frac{k}{k_\infty} = (1 + \gamma\theta)^n \quad (4.25)$$

$$C_p^* = \frac{C_p}{C_{p,\infty}} = (1 + \gamma\theta)^l \quad (4.26)$$

where $\gamma = \frac{T_w - T_\infty}{T_\infty}$ is the relative temperature difference parameter.

Transforming the governing equations to respective ODEs:

$$2f'''(1 + \gamma\theta)^m + ff'' \left(1 - \omega + \omega \frac{\rho_s}{\rho_f} \right) = 0 \quad (4.27)$$

$$\left(1 - \omega + \omega \frac{(\rho C_p)_s}{(\rho C_p)_f} \right) \left(\theta'' + \frac{Pr_\infty k_0 f \theta' (1 + \gamma\theta)^{l-n}}{2} \right) \quad (4.28)$$

$$- bk_1 R_H^* k_0 Pr_\infty \phi (1 + \gamma\theta)^{-n} = 0$$

$$\phi'' + \frac{f \phi' Sc_\infty}{2} - bk_1 Kr \phi Sc_\infty = 0 \quad (4.29)$$

where $R_H^* = \frac{R_H}{(\rho C_p)_f}$ is the reaction heat parameter and $Kr = \frac{C_\infty x}{U_\infty}$ is the chemical reaction parameter.

The boundary condition from Equation (4.17) is transformed to:

$$\left. \begin{aligned} f = f' = 0, \theta(0) = 1, \phi(0) = 1 \text{ as } \eta = 0 \\ f'(\infty) = 1, \theta(\infty) = 0, \phi(\infty) = 0 \text{ as } \eta = \infty \end{aligned} \right\} \quad (4.30)$$

4.3 Case Studies

4.3.1 Case I

Considering a mass fraction of particle of 0.1 and the mass fraction of gas of 0.9, i.e. $\omega = 0.1$, the equations reduce to the following:

$$f''' = -0.81ff''(1 + \gamma\theta)^{-m} \quad (4.31)$$

$$\theta'' = -\frac{Pr_\infty k_0 f \theta' (1 + \gamma\theta)^{l-n}}{2} - 0.4bk_1 R_H^* k_0 Pr_\infty \phi (1 + \gamma\theta)^{-n} = 0 \quad (4.32)$$

$$\phi'' + \frac{f\phi'Sc_\infty}{2} - bk_1 Kr\phi Sc_\infty = 0 \quad (4.33)$$

Equations (4.31) to (4.33) along with the boundary conditions from Equation (4.29) are solved for temperature ranges in the hydrolysis reaction with wall temperature of $T_w = 298 K$ and $T_\infty = 648 K$.

The Prandtl number is a determined by thermal conductivity, viscosity, and specific heat. Since these properties change within the boundary layer, Prandtl number also exhibits variation. Prior research [26, 30, 40] has shown that assuming a constant Prandtl number in the boundary layer, especially where thermophysical properties vary with temperature, yields inaccuracies. By considering the temperature-dependent variation of the Prandtl number:

$$Pr = \frac{\mu C_p}{k} = \frac{\mu_\infty (1 + \gamma\theta)^m C_{p,\infty} (1 + \gamma\theta)^l}{k_\infty (1 + \gamma\theta)^n} = (1 + \gamma\theta)^{m+l-n} Pr_\infty \quad (4.34)$$

Equation (4.32) can be expressed as:

$$\theta'' = -\frac{Pr k_0 f \theta' (1 + \gamma\theta)^{-m}}{2} - 0.4bk_1 R_H^* k_0 Pr \phi (1 + \gamma\theta)^{-m-l} = 0 \quad (4.35)$$

Similarly, the Schmidt number is defined by the ratio of viscous diffusivity and mass diffusivity and is represented as

$$Sc = \frac{\mu}{\rho D} = (1 + \gamma\theta)^m Sc_\infty \quad (4.36)$$

The equation representing species conservation, Equation (4.33), is stated as

$$\phi'' + \frac{f\phi'Sc(1 + \gamma\theta)^{-m}}{2} - bk_1Kr\phi Sc(1 + \gamma\theta)^{-m} = 0 \quad (4.37)$$

4.3.2 Case II

The hydrolysis reaction entails a higher steam to copper (II) chloride ratio for practical applications [38]. For this case, selecting the mass fraction of the particle to be 0.4 and the gas as 0.6, i.e. $\omega = 0.6$, the equation reduces to the following with variable Prandtl and Schmidt numbers:

$$f''' = -1.74ff''(1 + \gamma\theta)^{-m} \quad (4.38)$$

$$\theta'' - \frac{Prk_0f\theta'(1 + \gamma\theta)^{-m}}{2} - 0.14bk_1R_H^*k_0Pr\phi(1 + \gamma\theta)^{-m-l} = 0 \quad (4.39)$$

$$\phi'' + \frac{f\phi'Sc(1 + \gamma\theta)^{-m}}{2} - bk_1Kr\phi Sc(1 + \gamma\theta)^{-m} = 0 \quad (4.40)$$

The above equations, in conjunction with the boundary conditions from Equations (4.30), are solved for temperature ranges in the hydrolysis reaction with the wall temperature of $T_w = 298 K$ and $T_\infty = 648 K$.

The key physical parameters in this study include the Nusselt number, the skin-friction coefficient, and Sherwood number. These represent the rate of dimensionless rate of heat transfer, shear stress and rate of mass transfer, respectively.

The wall shear stress is expressed as

$$\tau_w = \mu \left[\frac{\partial u}{\partial y} \right]_{y=0} \quad (4.41)$$

The local skin friction coefficient (C_f) is

$$C_f Re_x^{1/2} = \frac{2\tau_w}{\rho U_\infty^2 x^2} = 2(1 + \gamma\theta)^m f''(0) \quad (4.42)$$

where Re_x is the local Reynolds number, $Re_x = \left(\frac{U_\infty x^2}{\nu} \right)$.

The Nusselt number can be represented as

$$Nu_x = \frac{xq''}{k(T_w - T_\infty)} \quad (4.43)$$

where the total surface / wall heat flux is the combination of radiative as well as conductive energy fluxes:

$$q'' = q_c'' + q_r'' \quad (4.44)$$

$$q'' = -k \left[\frac{\partial T}{\partial y} \right]_w - \frac{8\sigma^* T_\infty^3}{3k^*} \left[\frac{\partial T}{\partial y} \right]_w \quad (4.45)$$

An assumption is made that the approximation by Rosseland remains applicable at the wall [1].

Using Equations (4.44) and (4.45), Equation (4.43) can be expressed as

$$Nu_x Re_x^{-1/2} = -\theta'_w \left(1 + \frac{2}{3N_R} \right) \quad (4.46)$$

Similarly, defining a non-dimensional coefficient of mass transfer,

$$Sh = \frac{x D \left(\frac{\partial C}{\partial y} \right)_w}{(C_w - C_\infty)} \quad (4.47)$$

Similarly, defining a non-dimensional coefficient of mass transfer,

$$Sh Re_x^{-1/2} = -\phi'(0) \quad (4.48)$$

4.3.3 Case III Asymptotic Solutions

In this section, asymptotic analysis is done to study the expressions and behavior for different Prandtl numbers. In a wide range of applications, fluid Prandtl numbers are usually in the range of $0.1 < Pr < 1000$, so the solution is presented for three cases of Prandtl number, $Pr = 0.1, 10$ and 100 .

Small Prandtl Numbers

If the Prandtl number is small ($Pr \rightarrow 0$), the governing equation representing energy conservation from Equation (4.33) reduces to a different equation. Selecting a Prandtl number of 0.1, the following equation is obtained.

$$\theta'' - \frac{Pr k_0 f \theta' (1 + \gamma \theta)^{-m}}{2} = 0 \quad (4.49)$$

Equation (4.49) is subjected to the same boundary conditions imposed earlier.

Large Prandtl Numbers

When the Prandtl number is large ($Pr \rightarrow \infty$), the governing energy conservation equation from Equation (4.35) reduces to the following equation

$$\theta'' - \frac{Prk_0f\theta'(1 + \gamma\theta)^{-m}}{2} - 0.4bk_1R_H^*k_0Pr\phi(1 + \gamma\theta)^{-m-l} = 0 \quad (4.50)$$

This chapter aims to provide a better understanding of the physical interactions among these variables including temperature distribution and temperature gradient for different values of the radiation parameter, N_R . Similarly, the variations caused by the temperature dependency of various important parameters are examined, and asymptotic behaviour for varying Prandtl numbers are studied.

4.4 Results and Discussion

The equations are solved numerically with $\Delta\eta = 0.01$, employing a fourth-order shooting method, and a residual error less than 10^{-5} for all cases. Solutions are performed for a steam Prandtl number of 1, Schmidt number of 0.62 for water vapor, $Kr = 1$, $m = 0.66$, $n = 0.81$ and $l = 1$. The system of Equations (4.31), (4.35), and (4.37) is highly nonlinear and interdependent. A numerical solution for this equation set, considering the boundary conditions Eq. (4.30), is obtained using MATLAB.

Figure 4.1 shows the difference observed in the velocity profile when comparing the Blasius laminar flow with the chemically reacting flow of a solid-gas mixture and temperature dependent thermophysical properties. Cases when the radiation is absent are compared with two radiation parameter values. Thermal radiation does not influence the velocity profile distribution for the general case of Blasius flow as represented by the overlapping solid line where k_0 is the case without radiation and a radiation parameter of $N_R = 1$ and 0.3. However, due to the temperature dependency of dynamic viscosity in the fluid mixture in the momentum equation, the velocity profile increases with increment of radiation parameter. Figure 4.1 shows that the x-component of translational velocity increases with the increasing radiation parameter and fixed values of other

parameters. This signifies that velocity increases when moving away from the solid surface along the y-direction. This behaviour is a result of the fluid's interaction with a solid surface and the development of a boundary layer.

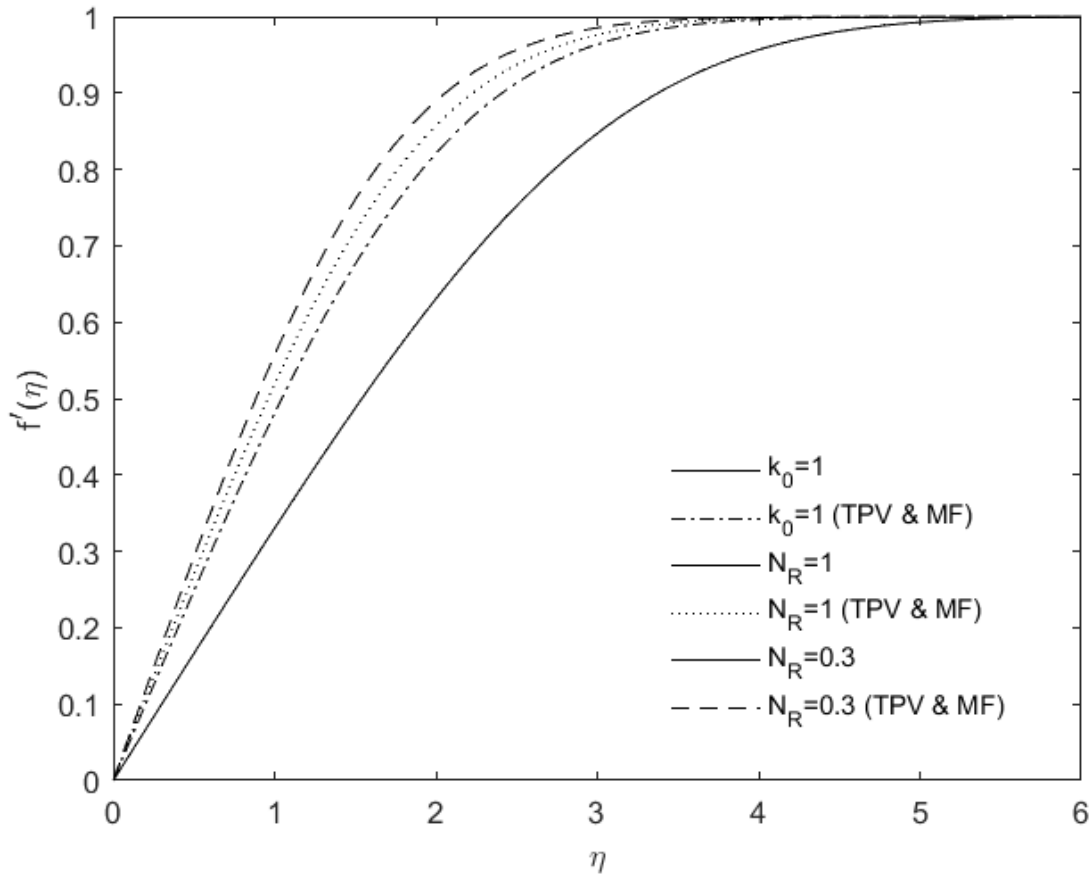


Figure 4.1 Velocity profile including thermophysical property variations and mass fraction of the mixture as a function of η in the presence of radiation ($N_R = 0.3$ and 1) and absence of radiation ($k_0 = 1$)

The presence of radiation causes a gradual change in fluid velocity with velocity highest for the maximum radiation case at $N_R = 0.3$. Similarly, considering the flow of a participating medium with solid particles along with the fluid causes a change in velocity profile. For $\eta = 1$, and $k_0 = 1$, there is approximately a 15% increase in the velocity profile caused by solid particles and

thermophysical property variations. Similarly, when a maximum radiation parameter of $N_R = 0.3$ is considered, the velocity profile increases by 24.3%. This signifies an enhancement in the hydrodynamic boundary layer thickness when solid particles are present in the flow and when temperature dependence of thermophysical property is incorporated.

The study of the temperature distribution shows the importance of incorporating the influence of temperature dependence and mixture properties in the model. It is observed that when specific heat capacity, thermal conductivity and viscosity depend on temperature, and the mass fraction of solids and fluid is considered, it narrows the temperature distribution. This reduction in the thickness of the boundary layer leads to a reduction in fluid temperature which may affect the reaction by favouring undesirable side reactions. This indicates that the temperature gradient near the reactor surface is steeper, implying a rapid change in temperature as the distance from the surface grows and heat transfer away from the reactor surface is more efficient. However, the inclusion of radiation improves the boundary layer thickness with the $\theta(\eta)$ value a maximum for the maximum radiation case of $N_R = 0.3$. This may also mean their effects in the boundary layer thickness can offset each other, to some extent. The temperature profile is noted to be consistently decreasing with the increase in η .

When $\eta = 1$, for no-radiation case, there is 6.9% decrease in the temperature profile due to the presence of solid particles in the fluid flow and the temperature dependent parameters. $N_R = 1$ causes a 5.8% decrease in the temperature profile. For a maximum radiation parameter of $N_R = 0.3$, the temperature profile decreases by 4.4%. Since the thermal radiation presence enhances heat transfer, the decrease of fluid temperature occurs with increase in thermal radiation. These insights on the effects of boundary layer thickness on temperature profiles are crucial for effective heat transfer and design for the hydrolysis process involving participating solid-gas flows.

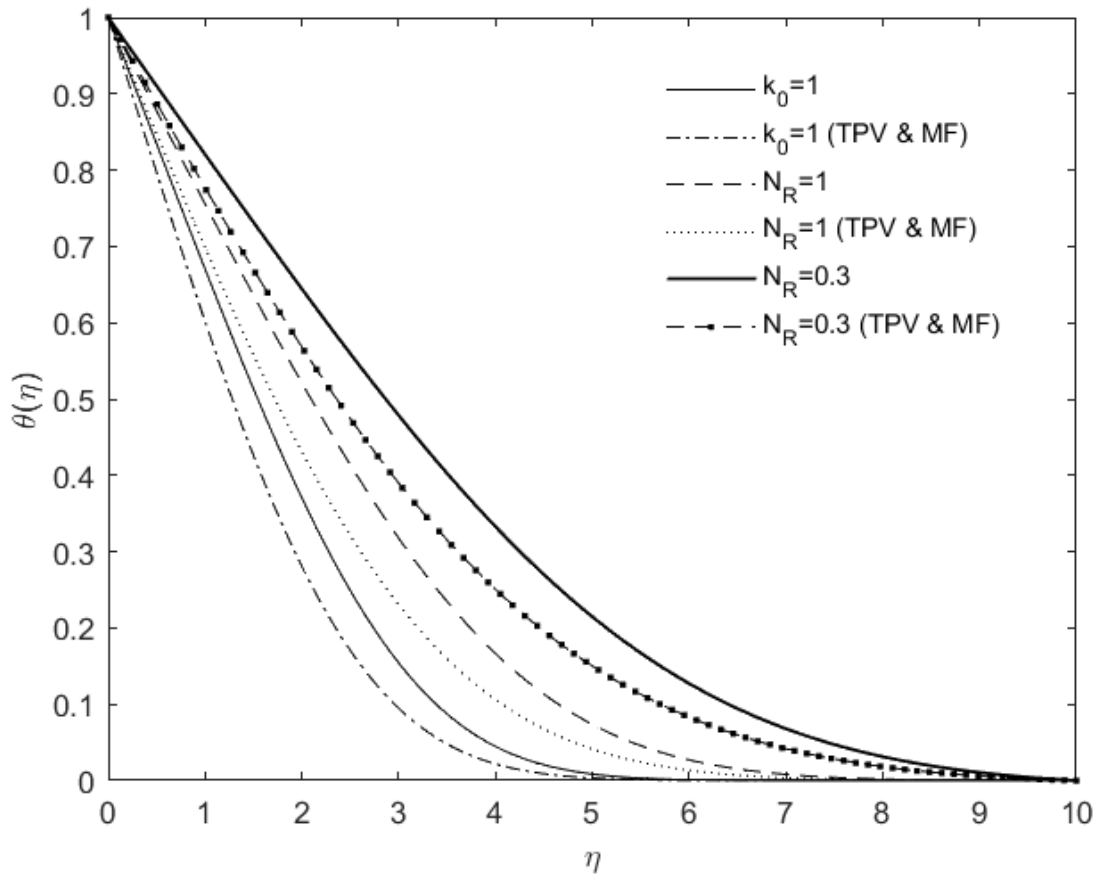


Figure 4.2 Temperature profile as a function of η including thermophysical property variations and mass fraction of the mixture in the presence of radiation ($N_R = 0.3$ and 1) and absence of radiation $k_0 = 1$

Figure 4.3 illustrates heat transfer variation within the boundary layer in relation to temperature gradient. Notably, the maximum temperature gradient is observed at a specific distance from the wall. The observed behavior is attributed to the non-linear relationship between radiant energy flux and temperature, as elucidated by the energy equation. The presence of radiation has a consequence of causing an increment in the temperature gradient compared to scenarios without radiation. Neglecting thermal radiation reduces the boundary layer thickness by 7.6%. In the transition to thermal radiation as the predominant heat transfer mode, denoted by a Nusselt number of 0.3, the temperature gradient at the wall diverges further from linearity with a decrease in the radiation

parameter. Additionally, the temperature-dependence of thermophysical properties and the mixture mass fraction contributes to an upsurge in the temperature gradient, regardless of the prevailing heat transfer modes. Observing the case with maximum radiation heat transfer, the effect of temperature dependence of Prandtl number is highly visible. Near the wall or boundary, a steeper gradient is in the presence and absence of radiation, indicating an increase of heat transfer. These variations in heat transfer depicted by the temperature gradient highlight the importance of investigating thermal radiation in temperature sensitive processes.

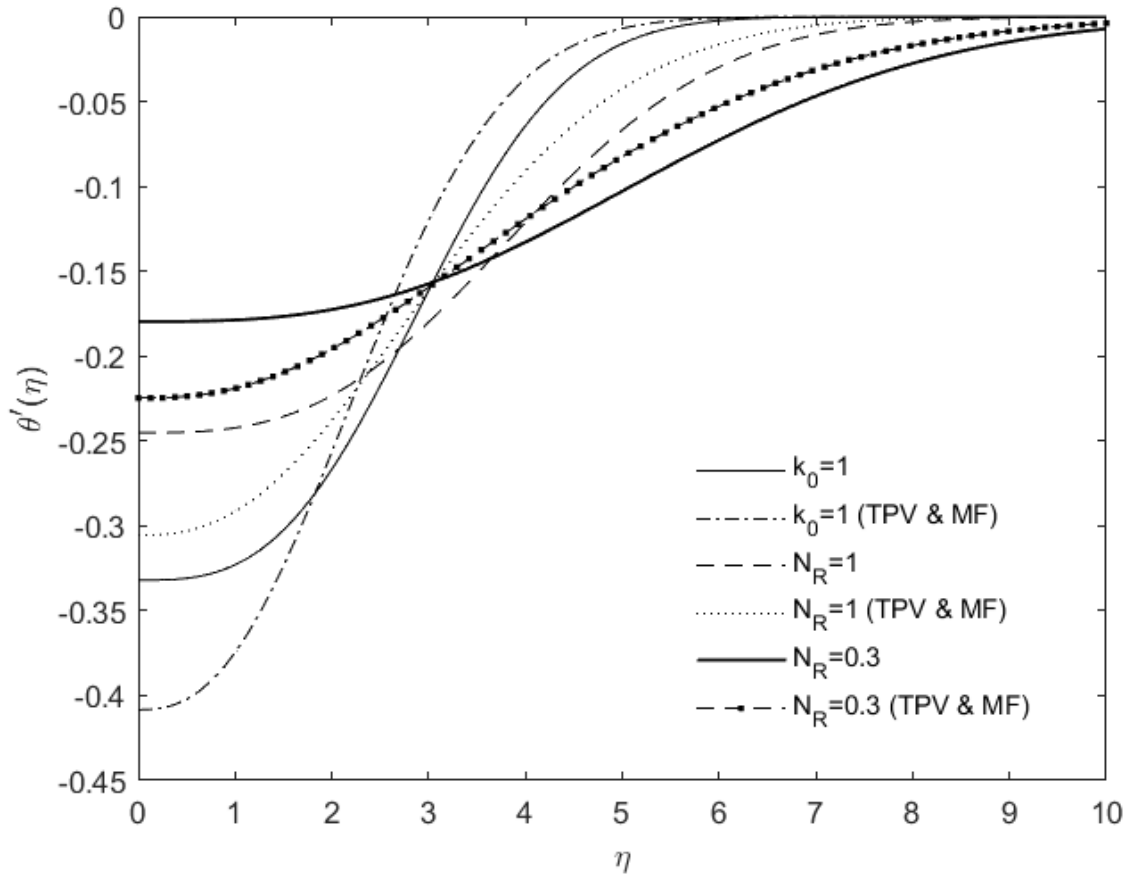


Figure 4.3 Temperature gradient across a boundary layer including thermophysical property variations and mass fraction of the mixture in the presence of radiation ($N_R = 0.3$ and 1) and absence of radiation $k_0=1$

Table 4.1 Heat transfer in flow along a plate represented as the local heat transfer parameter $(Nu_x Re_x^{-1/2})$

Radiation Parameter (N_R)	Case	$-\theta'(0)$ Blasius Flow	$-\theta'(0)$ with variable thermophysical properties and solid-gas flow
100	Thermal radiation neglected	0.332	0.408
1	Thermal radiation equal to conduction	0.245	0.305
0.3	Maximum radiation case	0.179	0.224

Table 4.1 provides the computed values of heat transfer rate for various radiation parameters. The heat transfer for the case of a general Blasius flow, also studied by Bataller [6], is compared with the case of a participating flow with a solid mass fraction of 0.1 and temperature dependent thermophysical properties. The results demonstrate that for solid-gas flow with a varying thermophysical properties, the heat transfer rate is appreciably affected by radiation.

As illustrated in Fig. 4.4, the temperature dependency of the Schmidt number changes the concentration profile. The concentration profile decreases with the rise of radiation parameter which indicates a faster convergence and higher extent of conversion in the reaction process. The graph also suggests that the endothermic chemical reaction has a crucial role in altering the chemical distribution in the boundary layer. The impact of solid mass fraction and variable thermophysical properties is evident, when $\eta = 1$, and $k_0 = 1$, with a 5% increment in the concentration. Equal radiative and conductive heat fluxes cause a 7.5% increase in concentration profile. For a maximum radiation case of $N_R = 0.3$, the concentration profile increases by 10.9%. The dotted line in the graph represents the concentration profile with a maximum radiation parameter of $N_R = 0.3$ when temperature dependence is considered.

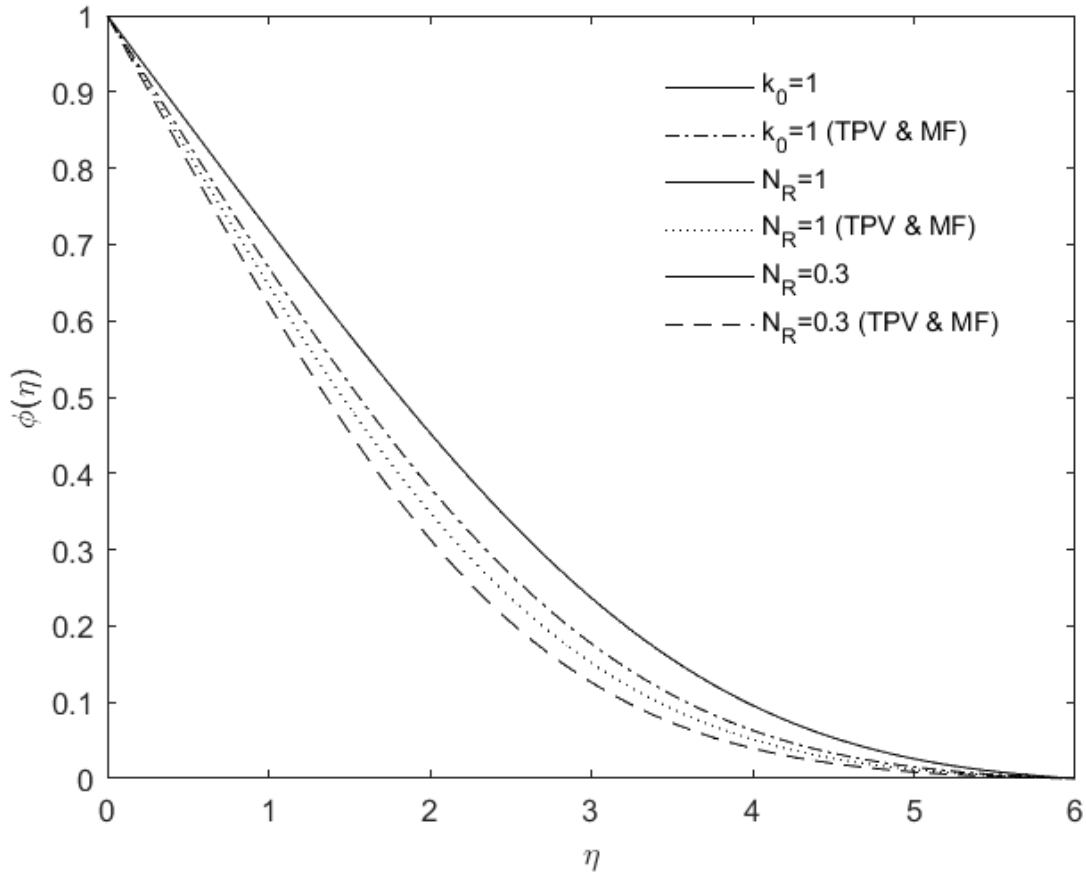


Figure 4.4 Concentration profile trends with respect to η including thermophysical property variations and mass fraction of the mixture in the presence of radiation ($N_R = 0.3$ and 1) and absence of radiation $k_0 = 1$

The inclusion of solid particles enhances heat and mass transfer and affects the concentration profile. This analysis of combined effects of radiation and with variable thermophysical properties in the participating solid-gas flow shows a reduction of concentration of the chemical species near the boundary / surface. Enhanced mass transfer and reaction rate, as well as changes in fluid properties with temperature promoting faster diffusion of species away from the boundary could be the leading cause. The fast-converging results in this case represent a higher extent of conversion of the solid particles.

Figures 4.5 to 4.7 represent the velocity profile, temperature gradient and concentration profile for a steam to copper (II) chloride ratio of 10, i.e., the particle mass fraction is 0.4. The velocity profile increases for increasing mass fraction of solid particles in the maximum radiation case of $N_R = 0.3$. This signifies the increase in fluid velocity when moving far from the solid surface along the y -direction for a hydrolysis reaction with a particle mass fraction of $\omega = 0.4$. The concentration profile decreases with an increasing particle mass fraction, indicating a faster convergence and higher extent of conversion in the reaction process.

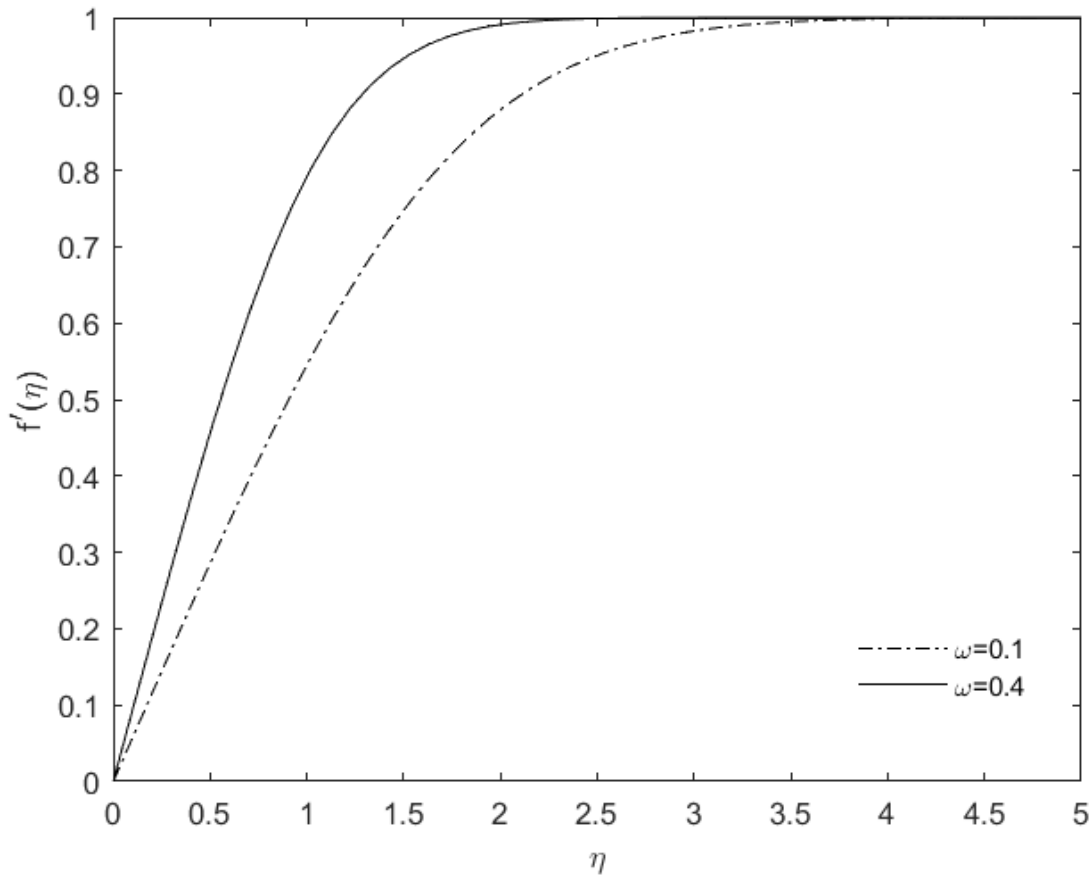


Figure 4.5 Velocity profile with varying solid particle mass fraction for a maximum radiation case

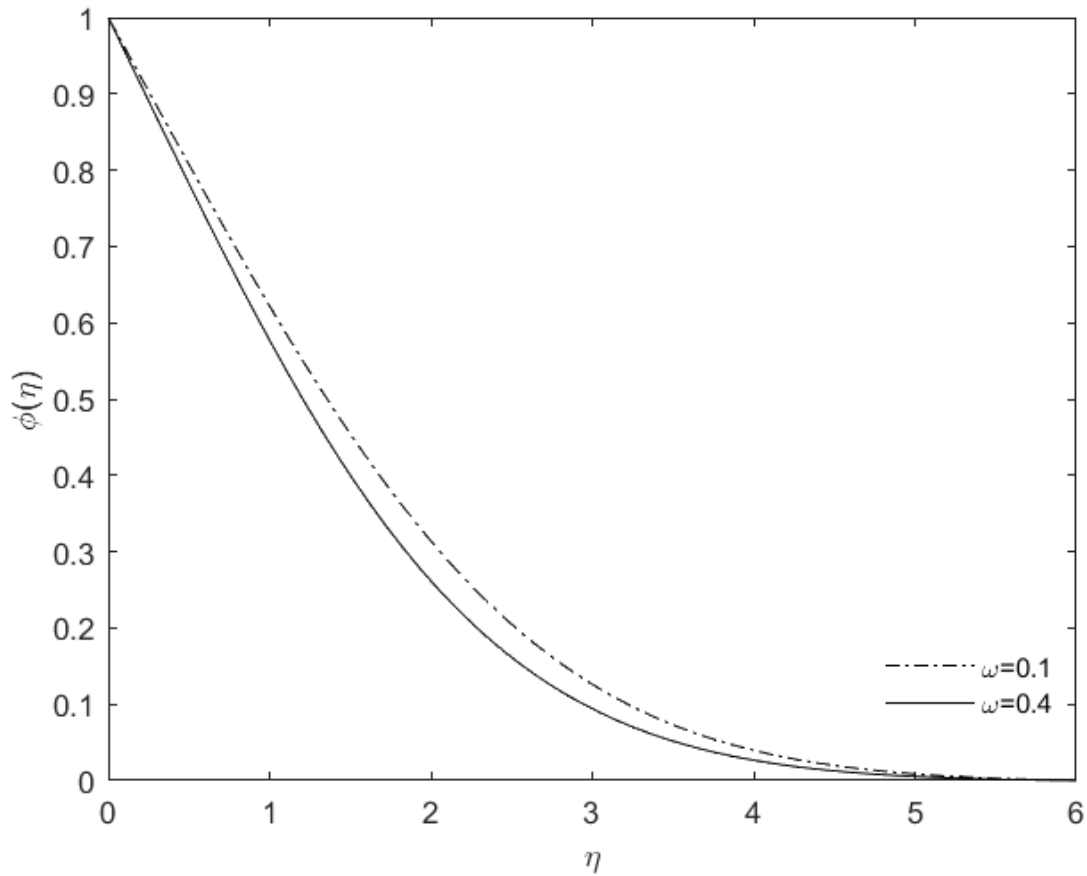


Figure 4.6 Concentration profile in the boundary layer with varying solid particle mass fraction for a maximum radiation case

Figure 4.7 illustrates a slight deviation in heat transfer for variable mass fraction when radiation is maximum. Enhanced heat transfer in the boundary layer flow is observed for $\omega = 0.4$. Consequently, it was noted that higher particle mass fractions led to improvements in both heat and mass transfer. $\theta'(\eta)$ represents the value of heat transfer for two mass fraction amounts and is presented in Figure 4.7.

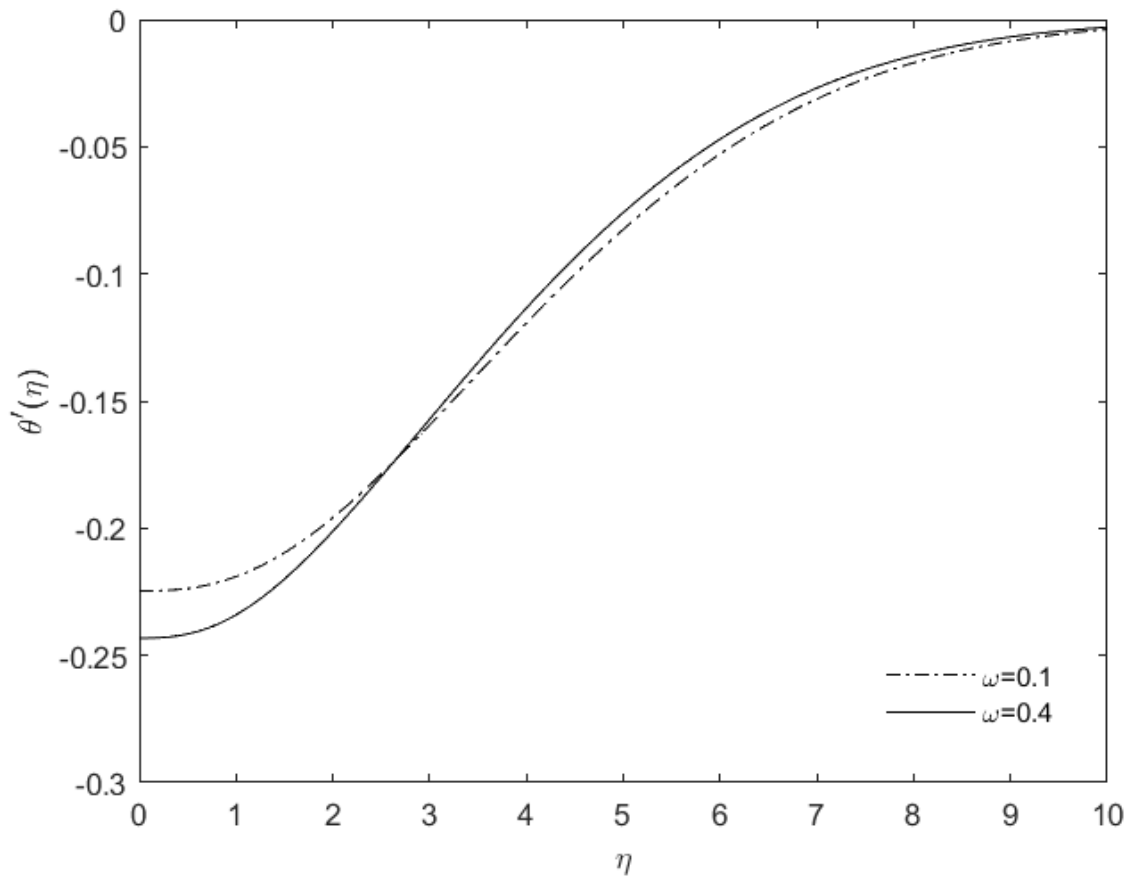


Figure 4.7 Temperature gradient across a boundary layer with varying solid particle mass fraction for a maximum radiation case

Similarly, a scaling analysis was performed to study the asymptotic behaviour for small and large Prandtl numbers. Numerical solutions are presented for Prandtl numbers 0.1, 10 and 100 for a case without radiation and compared against a radiation case with radiation parameter value $N_R = 0.3$. Figure 4.8 to 4.10 shows the velocity, temperature and concentration profile for respective cases.

Figure 4.8 illustrates the trends for variable Prandtl number for the cases when radiation is absent and when radiation is maximum. The velocity profile increases for decrease in Prandtl number for

both the cases. This signifies the increase in fluid velocity when moving far from the solid surface along the y -direction for a hydrolysis reaction with a Prandtl number of $Pr = 0.1$.

The deviation obtained for high and low Prandtl numbers for the maximum radiation case is less than that observed when $k_0 = 1$, indicating an increase in fluid velocity at lower Prandtl numbers. It also highlights that the heat diffuses more quickly compared to the velocity when maximum radiation is present.

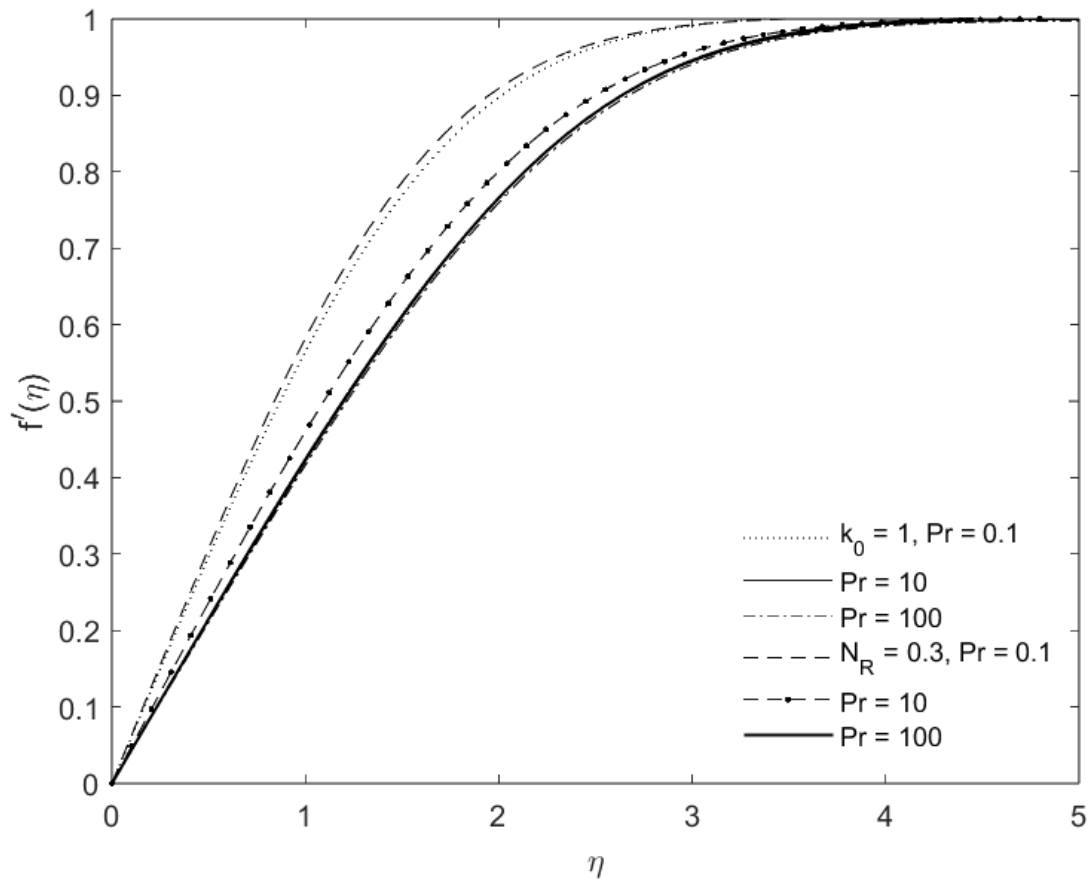


Figure 4.8 Velocity profile across a boundary layer with varying Prandtl numbers at $k_0 = 1$ and $N_R = 0.3$

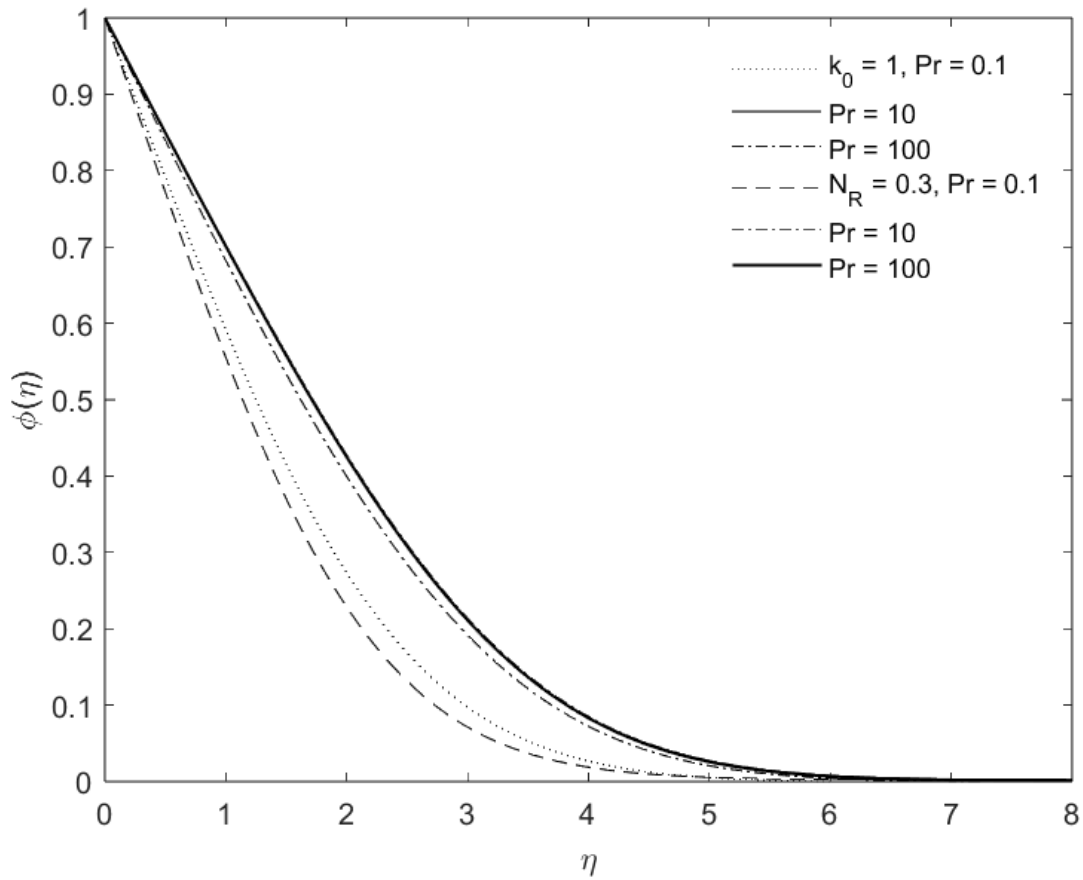


Figure 4.9 Concentration profile across a boundary layer with varying Prandtl number at $k_0 = 1$ and $N_R = 0.3$

Figure 4.9 presents the asymptotic concentration profile trends for two distinct cases. Faster conversion is observed for cases where Prandtl number is small i.e. $Pr = 0.1$ with an increase in conversion when radiation is maximum. Similarly, a distinct asymptotic behaviour is observed for large Prandtl numbers at $k_0 = 1$ and $N_R = 0.3$ as presented in Figure 4.10. Improvement in the boundary layer thickness was observed for $Pr = 0.1$ with the thickness increasing with radiation parameter which also signifies an improvement in heat transfer.

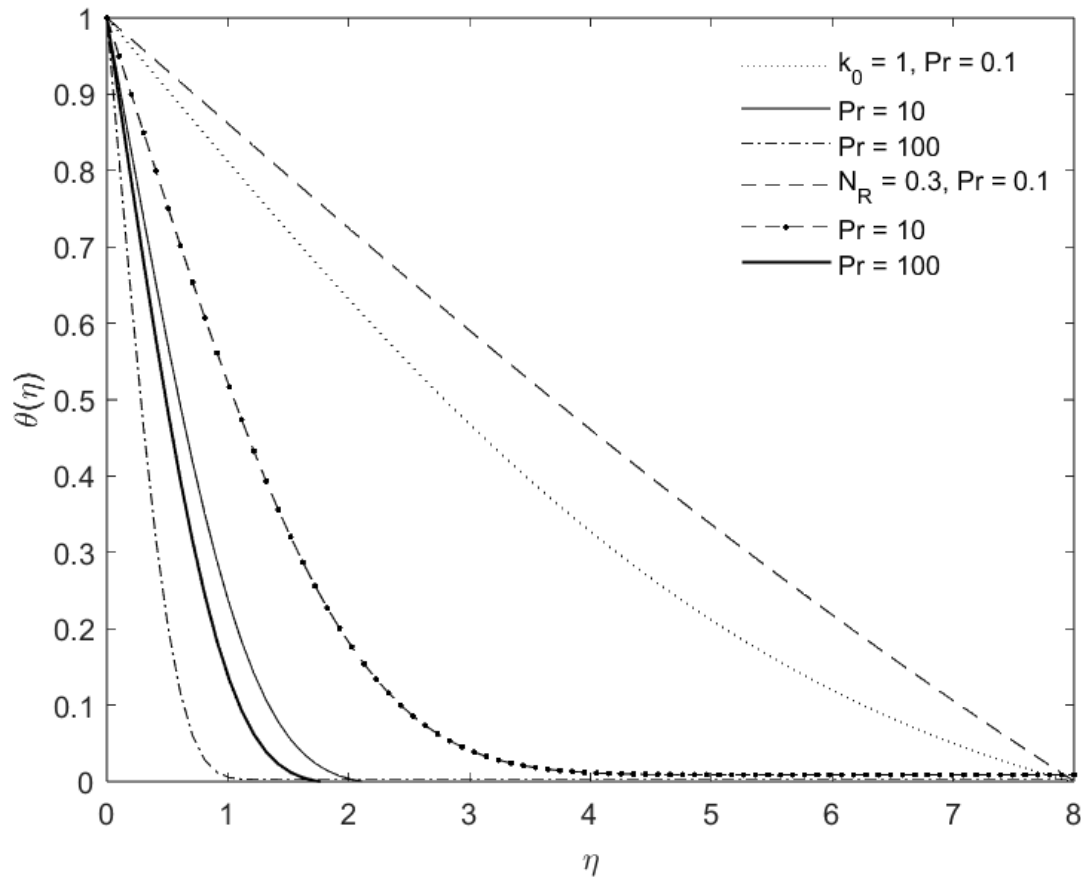


Figure 4.10 Temperature profile across a boundary layer with varying Prandtl number at $k_0 = 1$ and $N_R = 0.3$

4.5 Conclusions

This chapter explores the laminar boundary layer flow with thermal radiation influence in a participating solid-gas flow with variable thermophysical properties. The conversion of partial differential equations into governing ordinary differential equations was achieved using similarity variables. The solution was obtained using a fourth-order Runge-Kutta shooting technique. Numerical results include the temperature profile and the concentration profile, along with temperature gradients within the boundary layer. The research demonstrated a notable influence

of radiation in the boundary layer flow during hydrolysis reaction. With higher radiation parameters, the thermal boundary layer thickness improved. The results showed the significance of accounting for temperature dependency of the chemical reaction rate constant in the reactor, as well as variable thermophysical properties.

The endothermic chemical reaction led to an increment in the thermal boundary layer thickness. The temperature dependence of thermophysical properties and mixture mass fraction caused a change in the temperature gradient regardless of the modes of heat transfer. The inclusion of solid particles enhanced the heat and mass transfer and affected the concentration profile. The investigation into the collective effects of thermal radiation and variable thermophysical properties showed a decrease in the concentration of chemical species near the surface / boundary. Similarly, the temperature and concentration profiles suggested increased mass and heat transfer rates when the particle mass fraction in the flow was 0.4. The results of this study highlight the importance of thermal radiation in temperature sensitive reactions. It also provides useful insights on the velocity profiles, the temperature profiles and concentration profiles, along with the temperature gradient for a comprehensive understanding of heat and mass transfer processes in the hydrolysis process.

References

- [1] Y. A. Cengel, and A. J. Ghajar, "Heat transfer," McGraw-Hill education, New York, NY, 2018.
- [2] W. J. Smith, "Effect of gas radiation in the boundary layer on aerodynamic heat transfer," *Journal of the aeronautical sciences*, vol. 20, pp. 579-580, 1952.
- [3] R. Viskanta, and R. J. Grosh, "Boundary layer in thermal radiation absorbing and emitting media," *International journal of heat and mass transfer*, vol. 5, no. 9, pp. 795-806, 1962.

- [4] J. T. Howe, "Radiation shielding of the stagnation region of an opaque gas," NASA technical note D-329, 1960.
- [5] L. P. Kadanoff, "Radiative transport within an abating body," *Transactions of ASME journal of heat transfer*, vol. C83, pp. 215-225, 1961.
- [6] R. Bataller, "Radiation effects in Blasius flow," *Applied Mathematics and Computation*, vol. 198, no. 1, pp. 333-338, 2008.
- [7] A. Raptis, C. Perdakis, and H. S. Takhar, "Effect of thermal radiation on MHD flow," *Applied mathematics and computation*, vol. 153, no. 3, pp. 645-649, 2004.
- [8] P. K. Tripathy, T. Samantara, J. Mishra, and S. Panda, "Mixed convective radiative heat transfer in a particle-laden boundary layer fluid over an exponentially stretching permeable surface," *AIP conference proceedings*, vol. 2435, 2022.
- [9] S. M. Ibrahim, and N. B. Reddy, "Similarity solution of heat and mass transfer for natural convection over a moving vertical plate with internal heat generation and a convective boundary condition in the presence of thermal radiation, viscous dissipation, and chemical reaction," *ISRN thermodynamics*, 2013.
- [10] M. A. Hossain, and H. S. Takhar, "Radiation effect on mixed convection along a vertical plate with uniform surface temperature," *Heat and mass transfer*, vol. 31, pp. 243-248, 1996.
- [11] N. C. Roy, S. Masud, S. Parvin, S. Roy, and R. P. Sharma, "Impact of variable thermo-physical properties on the combustion of a gas mixture past an axisymmetric body with thermal radiation," *Cleaner engineering and technology*, vol. 4, 2021.

- [12] B. L. Kuo, "Heat transfer analysis for the Falkner-Skan wedge flow by the differential transformation method," *International journal of heat and mass transfer*, vol. 48, no. 23-24, pp. 5036-5046, 2005.
- [13] A. J. Chamkha, and J. Peddieson Jr., "Boundary layer flow of a particulate suspension past a flat plate," *International journal of multiphase flow*, vol. 17, pp. 805-808, 1991.
- [14] S. K. Mishra, and P. K. Tripathy, "Numerical investigation of free and forced convection two-phase flow over a wedge," *AMSE: Journal of thermal science and engineering applications*, vol. 82, pp. 92, 2013.
- [15] M. Ferdows, and M. Q. Al-Mdallal, "Effects of Order of Chemical Reaction on a Boundary Layer Flow with Heat and Mass Transfer Over a Linearly Stretching Sheet," *American journal of fluid dynamics*, vol. 2, no. 6, pp. 89-94, 2013.
- [16] M. Hussain, Q. A. Ranjha, M. S. Anwar, S. Jahan, and A. Ali, "Eyring-Powell model flow near a convectively heated porous wedge with chemical reaction effects," *Journal of the Taiwan institute of chemical engineers*, vol. 139, 2022.
- [17] H. Schlichting, "Boundary Layer Theory," 2nd edition, Pergamon press, New York, 1955.
- [18] O. D. Makinde, "On MHD boundary-layer flow and mass transfer past a vertical plate in a porous medium with constant heat flux," *International journal of numerical methods for heat & fluid flow*, vol. 19, no. 3/4, 2009.
- [19] J. Chamkha, "Thermal radiation and buoyancy effects on hydromagnetic flow over an accelerating surface with heat source or sink plate embedded in a thermally stratified porous

medium with Hall effects,” *International journal of engineering science.*, vol. 38, pp. 2689-2701, 2000.

[20] C. H. Chen, “Combined heat and mass transfer in MHD free convection from a vertical surface with Ohmic heating and viscous dissipation,” *International journal of engineering science*, vol. 42, no. 7, pp. 699-713, 2004.

[21] O. D. Makinde, “Similarity solution for natural convection from a moving vertical plate with internal heat generation and a convective boundary condition,” *Thermal science*, vol. 15, 2011.

[22] L. J. Crane, “Flow past a stretching plate,” *ZAMP*, vol. 21, pp. 645-647, 1970.

[23] E. M. A. Elbashbeshy, “Heat transfer over a stretching surface with variable heat flux,” *Journal of physics D: applied physics*, vol. 31, pp. 1951-1955, 1998.

[24] M. S. Abel, and N. Mahesha, “Heat transfer in MHD viscoelastic fluid flow over a stretching sheet with variable thermal conductivity, non-uniform heat source and radiation,” *Applied mathematical modelling*, vol. 32, pp. 1965-1983, 2008.

[25] M. M. Rahman, and K. M. Salahuddin, “Study of hydromagnetic heat and mass transfer flow over an inclined heated surface with variable viscosity and electric conductivity,” *Communications in nonlinear science and numerical simulation*, vol. 15, pp. 2073-2085, 2010.

[26] M. M. Rahman, “Combined effects of internal heat generation and higher order chemical reaction on the non-Darcian forced convective flow of a viscous incompressible fluid with variable viscosity and thermal conductivity over a stretching surface embedded in a porous medium,” *Canadian journal of chemical engineering*, vol. 90, no. 6, pp. 1632-1645, 2012.

- [27] M. A. Lewis, M. Serban, and J. K. Basco, "Nuclear production of hydrogen, second information exchange meeting Argonne," *Argonne, Illinois: Argonne National Laboratory*, pp. 145-156, 2003.
- [28] R. M. Kasmani, S. Sivasankaran, M. Bhuvaneswari, and Z. Siri, "Effect of chemical reaction on convective heat transfer of boundary layer flow in nanofluid over a wedge with heat generation / absorption and suction," *Journal of applied fluid mechanics*, vol. 9, no. 1, pp. 379-388, 2016.
- [29] E. K. Luckins, J. M. Oliver, C. P. Please, B. M. Sloman, and R. A. Van Gorder, "Modelling and analysis of an endothermic reacting counter-current flow," *Journal of fluid mechanics*, pp. 947-949, 2022.
- [30] A. Pantokratoras, "The Falkner–Skan flow with constant wall temperature and variable viscosity," *International journal of thermophysics*, vol. 45, pp. 378-389, 2006.
- [31] M. M. Rahman, A. Aziz, and M. Al-Lawatia, "Heat transfer in micropolar fluid along an inclined permeable plate with variable fluid properties," *International journal of thermophysics*, vol. 49, pp. 993-1002, 2010.
- [32] S. R. Tieszen, "On the fluid mechanics of fires," *Annual review fluid mechanics*, vol. 33, no. 1, pp. 67-92, 2001.
- [33] S. K. Mishra, and P. K. Tripathy, "Mathematical and numerical modeling of two-phase flow and heat transfer using non-uniform grid," *Far East journal of applied mathematics*, vol. 54, pp. 107-126, 2011.

- [34] H. Xu, "A homogeneous-heterogeneous reaction model for heat fluid flow in the stagnation region of a plane surface," *International communications in heat and mass transfer*, vol. 87, pp. 112-117, 2017.
- [35] G. F. Naterer, I. Dincer, and C. Zamfirescu, "Hydrogen production from nuclear energy," Springer, New York, NY, 2013.
- [36] D. Thomas, N. A. Baveja, K. T. Shenoy, and J. B. Joshi, "Experimental study on the mechanism and kinetics of CuCl_2 hydrolysis reaction of the Cu-Cl thermochemical cycle in a fluidized bed reactor," *Industrial and engineering chemistry research*, vol. 59, no. 26, pp. 12028-12037, 2020.
- [37] A. Farsi, I. Dincer, and G. F. Naterer, "Particle formation and heat transfer in a gas-solid hydrolysis reactor with cupric chloride conversion to copper oxychloride," *International journal of heat and mass transfer*, vol. 161, 2020.
- [38] K. Pope, Z. L. Wang, and G. F. Naterer, "Process integration of material flows of copper chlorides in the thermochemical Cu-Cl cycle," *Chemical engineering research and design*, vol. 109, pp. 273-281, 2016.
- [39] C. Zamfirescu, I. Dincer, and G. F. Naterer, "Thermophysical properties of copper compounds in copper – chlorine thermochemical water splitting cycles," *International journal of hydrogen energy*, vol. 35, no. 10, pp. 4839-4852, 2010.
- [40] V. N. Daggupati, G. F. Naterer, and K. S. Gabriel, "Diffusion of gaseous products through a particle surface layer in a fluidized bed reactor," *International journal of heat and mass transfer*, vol. 53, no. 11-12, pp. 2449-2458, 2010.

- [41] S. Rosseland, “Astrophysics on an atomic theoretical basis,” vol. 42, Springer, Berlin, 1931.
- [42] D. M. Tellep and D. K. Edwards, “Radiant energy transfer in gaseous flows,” *Lockheed missile and space division*, LMSD-288203, 1960.
- [43] R. Viskanta, “Heat transfer in thermal radiation absorbing and scattering media,” ANL-6170, 1960.
- [44] G. F. Naterer, “Advanced heat transfer,” 3rd edition, CRC Press, Boca Raton, FL, 2021.

Chapter 5 – Conclusions and Recommendations

Hydrogen is a promising pathway to meet the world's increasing energy demand while reducing greenhouse gas emissions. While there are various hydrogen production techniques, thermochemical water splitting cycles such as the Cu-Cl cycle can reduce emissions compared to other traditional approaches [1]. The hydrolysis step represents a particularly challenging aspect of the Cu-Cl cycle [2, 3]. It is recognized that when chemical reactions occur within a fluid flow, there can be a substantial impact on the overall rates of mass and heat transfer. Conversely, transport phenomena can significantly affect the overall rates of reactant conversion [4]. Better understanding of the heat and mass transfer during the process is crucial for improving the overall cycle efficiency and large-scale production.

In this thesis, impacts of thermal radiation on fluid flow in a hydrolysis reaction have been presented to gain a better understanding on the transport phenomena in the hydrolysis reactor. A semi-analytical model is presented with a Rosseland's radiation approximation [6]. The model is first validated by a previously established benchmark problem and then extended to report the effects of radiation and changes in specific heat and the chemical reaction constant. It is reported that during the hydrolysis reaction, it is crucial to account for temperature dependency of the chemical reaction rate constant and the thermophysical properties. The thickness of the thermal boundary layer was observed to be increasing with the impact of higher radiation parameters.

Past studies have reported the thermophysical properties of copper compounds in the Cu-Cl cycle [5]. Maxwell's power law studied the temperature dependent thermophysical properties at a temperature of 375 °C and copper (II) chloride mass fraction of 0.1 and 0.4. Analysis of different cases emphasized a noticeable role of radiation in the boundary layer flow. The presence of solid particles enhances the heat and mass transfer and affects the concentration profile. The study

presented in this thesis also showed that the effect of a chemical reaction on the thermal boundary layer is minimized in the presence of thermal radiation. Examining the combined influence of thermal radiation and varying thermophysical properties revealed a decrease in the concentration of chemical species near the surface. This is attributed to an enhanced mass transfer rate, an increased reaction rate, or changed fluid properties with temperature to promote faster diffusion of species away from the boundary layer.

This study highlighted a gap of knowledge regarding boundary layer transport phenomena in the hydrolysis step and the significance of thermal radiation. Overall, this model identified the impact of radiation heat transfer in the thermal boundary layer and fluid flow and presented the influence of chemical reactions and temperature-dependent thermophysical properties in the hydrolysis process.

5.1 Future Recommendations

Thermal radiation represents a relatively underexplored subject for the hydrolysis process. The insights from this study provide a new perspective on the laboratory experimental studies. Additional research is recommended to have a better understanding of the transport phenomena within the process. Future recommendations for this work are summarized as follows.

- The present modeling is conducted on a flat surface. This could be extended to more complicated geometries.
- Detailed study on emissivity, reflectivity and absorptivity could enhance the model.
- In the existing model, Maxwell's power law is used to account for variations in thermophysical properties. Further exploration of these thermophysical properties could provide valuable enhancements to the existing model.

- The semi-analytical model in this thesis assumed two-dimensional boundary layer flow across the surface. Integration of the third dimension could enhance the model and provide further insights.
- Due to limited experimental data in the boundary layer in published literature, conducting experimental research related to boundary layer heat and fluid flow would also enhance the numerical model by offering valuable data for validation.
- Further study can be performed on the thermochemistry changes within the boundary layer, providing further insights in the heat and mass transfer processes in hydrolysis.

References

- [1] B. W. Mcquillan *et al.*, “High efficiency generation of hydrogen fuels using solar thermal-chemical splitting of water (Solar thermo-chemical splitting for H₂),” 2010.
- [2] G. F. Naterer, I. Dincer, and C. Zamfirescu, “Hydrogen production from nuclear energy,” Springer, New York, NY, 2013.
- [3] D. Thomas, N. A. Baveja, K. T. Shenoy, and J. B. Joshi, “Experimental study on the mechanism and kinetics of CuCl₂ hydrolysis reaction of the Cu-Cl thermochemical cycle in a fluidized bed reactor,” *Industrial and engineering chemistry research*, vol. 59, no. 26, pp. 12028-12037, 2020.
- [4] H. Xu, “A homogeneous-heterogeneous reaction model for heat fluid flow in the stagnation region of a plane surface,” *International communications in heat and mass transfer*, vol. 87, pp. 112-117, 2017.
- [5] C. Zamfirescu, I. Dincer, and G. F. Naterer, “Thermophysical properties of copper compounds in copper – chlorine thermochemical water splitting cycles,” *International journal of hydrogen energy*, vol. 35, no. 10, pp. 4839-4852, 2010.

[6] S. Rosseland, “Astrophysics on an atomic theoretical basis,” vol. 42, Springer, Berlin, 1931.

Appendix A: MATLAB Codes

Maximum Radiation Model ($N_R = 0.3$) – Function and Script

```
function D = Nr3a12(~, C)

% viscosity constant, thermal conductivity constant and specific constant

l = 1; % From Rahman

m = 0.666;

n = 0.81;

%F0 = C(1); f

dF0deta = C(2); %f

dF1deta = C(3); %f'

%theta0 = C(4); %theta

gamma = -0.933; %gamma = (Tw-Tinf)/Tinf = -350/375 = -0.933

dF2deta = (-0.81*C(1)*C(3)*(1+gamma*C(4))^-m); %f'''

dtheta0deta = C(5); %theta'

%phi=C(6); %phi

dphi0deta=C(7); %phi'

Pr = 1;

k0=0.1837; %NR=0.3

%Rh = 1; %arbitrary value

Rhstar = 0.0000587; % Rhstar=Rh/(rho*Cp)f = 1/(472.6*36) % Reaction heat parameter

(mol·s2/m3)
```

```
dtheta1deta = -(0.5*Pr*k0*C(1)*C(5)*(1+gamma*C(4))^(-m)+(19354.8*exp(-5391.09*(-
350*C(4)+648))*Rhstar*Pr*(1+gamma*C(4))^(-m-1)*k0*C(6)); %%solid mass fraction=0.1
```

```
Sc = 0.62; %Schmidt number for water vapour
```

```
Kr = 1; %Reaction Constant
```

```
dphi1deta = -(0.5*C(1)*C(7)*Sc*(1+gamma*C(4))^(-m)+(48000*exp(-5391.09*(-
350*C(4)+648))*Kr*C(6)*Sc*(1+gamma*C(4))^(-m));
```

```
D = [dF0deta; dF1deta; dF2deta; dtheta0deta; dtheta1deta; dphi0deta; dphi1deta];
```

```
end
```

```
%To correctly determine the initial values
```

```
clear;
```

```
clc;
```

```
close all;
```

```
eta = linspace(0,8,80);
```

```
cinit = [0;0;0.5;1;-0.2;1;-0.4]; %f,f',theta,theta',phi,phi'
```

```
%%Initial value guesses :phi= -0.3 and -0.4; theta= -0.2 and -0.3; f'= 0.5 and 0.6
```

```
[eta,C] = ode45(@Nr3a12,eta,cinit)
```

```
figure(1); plot (eta,C(:,4));
```

```
xlabel('\eta');
```

```
ylabel('theta');
```

```
figure(2); plot (eta,C(:,6));
```

```
xlabel('\eta');  
ylabel('phi');  
figure(3); plot (eta,C(:,2));  
xlabel('\eta');  
ylabel('f');
```

Plots

%Forth order Runge-Kutta Shooting Method and Plots

```
close all;  
clear;  
clc;  
  
eta = linspace(0,10,80);  
n1 = 0.5; %f'guess  
n2 = 0.6;  
    h1 = -0.2; %%theta' guesses  
    h2 = -0.3;  
e1 = -0.3; %%phi' guesses  
e2 = -0.4;  
err_threshold = 0.00001; %for  
err_2 = 0.00001; %%for theta'  
err_3 = 0.00001; %%for phi'  
iterator = 1;
```

```

err = 1;

err2 = 1;

err3 = 1;

while err>err_threshold && err2>err_2 && err3>err_3

    if iterator == 1

        [eta,H] = ode45(@Nr3a12,eta,[0;0;n1;1;h1;1;e1]);

        o1 = H(end,2);

        f1 = H(end,4);

        g1 = H(end,6);

        %

        [eta,H] = ode45(@Nr3a12,eta,[0;0;n2;1;h2;1;e2]);

        o2 = H(end,2);

        f2 = H(end,4);

        g2 = H(end,6);

        figure (8); plot(n1,o1,'ok',n2,o2,'ok')

        figure(9); plot(h1,f1,'ok',h2,f2,'ok')

        figure(10); plot(e1,g1,'ok',e2,g2,'ok')

    else

        n2 = ((1-o1)*((n2-n1)/(o2-o1)))+n1;

        h2 = ((0-f1)*((h2-h1)/(f2-f1)))+h1;

        e2 = ((0-g1)*((e2-e1)/(g2-g1)))+e1;

        [eta,H] = ode45(@Nr3a12,eta,[0;0;n2;1;h2;1;e2]);

        o2 = H(end,2);

```

```

f2 = H(end,4);
g2 = H(end,6);
figure(8);hold on;plot(n2,o2,'or')
figure(9);hold on;plot(h2,f2,'or')
figure(10);hold on;plot(e2,g2,'or')

err = abs(1-o2);
err2 = abs(0-f2);
err3 = abs(0-g2);

end

iterator = iterator+1;

end

disp('Value of fdd with mass fraction and thermophysical property variation and radiation factor
Nr=0.3 is =');disp(n2);

disp ('Value of fd with mass fraction and thermophysical property variation and radiation factor
Nr=0.3 is =')disp(o2);

disp('Value of thetad with mass fraction and thermophysical property variation and radiation
factor Nr=0.3 is ='); disp(h2);

disp('Value of theta with mass fraction and thermophysical property variation and radiation
factor Nr=0.3 is ='); disp(f2);

disp('Value of phid with mass fraction and thermophysical property variation and radiation factor
Nr=0.3 is ='); disp(e2);

disp('Value of phi with mass fraction and thermophysical property variation and radiation factor
Nr=0.3 is ='); disp(g2);

```

```

figure(4),hold on; plot(eta, H(:,6),'--k')
ylabel('\phi(\eta)')
ylim([0 1])
xlabel('\eta')
legend('k_0=1','k_0=1 (TPV & MF)','N_R=1','N_R=1 (TPV & MF)','N_R=0.3','N_R=0.3 (TPV
& MF)','location','best')
legend boxoff
%legend('k0=1','NR=0.7,");
figure(5),hold on; plot(eta, H(:,4),'--k')
ylabel('\theta(\eta)')
ylim([0 1])
xlabel('\eta')
legend('k_0=1','k_0=1 (TPV & MF)','N_R=1','N_R=1 (TPV & MF)','N_R=0.3','N_R=0.3 (TPV
& MF)','location','best')
legend boxoff
figure(6),hold on; plot(eta, H(:,5),'--k')
ylabel('\theta^\prime(\eta)')
xlabel('\eta')
ylim ([-0.45 0])
legend('k_0=1','k_0=1 (TPV & MF)','N_R=1','N_R=1 (TPV & MF)','N_R=0.3','N_R=0.3 (TPV
& MF)','location','best')
legend boxoff
figure(7),hold on; plot(eta, H(:,2),'--k')

```

```
ylabel('f^\prime(\eta)')
```

```
xlabel('\eta')
```

```
ylim([0 1])
```

```
legend('k_0=1','k_0=1 (TPV & MF)','N_R=1','N_R=1 (TPV & MF)','N_R=0.3','N_R=0.3 (TPV  
& MF)','location','best')
```

```
legend boxoff
```